

(12) LEVEL

DDC FILE COPY
A066253

Technical Note

1978-29

[Handwritten signature]

R. J. Sasiela

The Monopulse Performance
of an Optical Heterodyne Detector
with Varying LO Distributions

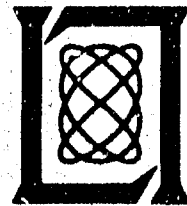
21 December 1978

Prepared for the Defense Advanced Research Projects Agency
under Electronic Systems Division Contract F19628-78-C-0002 by

Lincoln Laboratory

MASSACHUSETTS INSTITUTE OF TECHNOLOGY

LEXINGTON, MASSACHUSETTS



Approved for public release; distribution unlimited.

DDC
RECEIVED
MAR 23 1979

REPRODUCED FROM
BEST AVAILABLE COPY

79 03 22 043

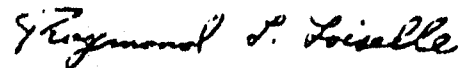
The work reported in this document was performed at Lincoln Laboratory, a center for research operated by Massachusetts Institute of Technology. This work was sponsored by the Defense Advanced Research Projects Agency under Air Force Contract F19628-78-C-0002 (ARPA Order 600).

This report may be reproduced to satisfy needs of U.S. Government agencies.

The views and conclusions contained in this document are those of the contractor and should not be interpreted as necessarily representing the official policies, either expressed or implied, of the United States Government.

This technical report has been reviewed and is approved for publication.

FOR THE COMMANDER



Raymond L. Loisel, Lt. Col., USAF
Chief, ESD Lincoln Laboratory Project Office

MASSACHUSETTS INSTITUTE OF TECHNOLOGY
LINCOLN LABORATORY

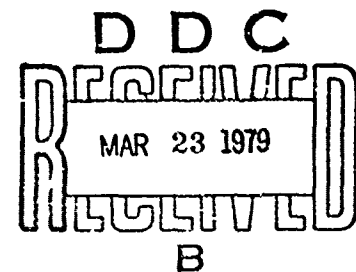
THE MONOPULSE PERFORMANCE
OF AN OPTICAL HETERODYNE DETECTOR
WITH VARYING LO DISTRIBUTIONS

R. J. SASIELA

Group 54

TECHNICAL NOTE 1978-29

21 DECEMBER 1978



Approved for public release; distribution unlimited.

LEXINGTON

MASSACHUSETTS

79 03 22 043

ABSTRACT

Calculations are performed to determine the monopulse characteristics, the signal-to-noise ratio, efficiency, and the transmit-receive pattern of an optical heterodyne detector composed of four quadrants. The variation of these quantities for a varying receive beam size on the detector, and a uniform LO, and Gaussian and Airy LO distributions of varying size are tabulated.

The calculations are applied to determine the possibility of increasing the angular coverage of an optical heterodyne receiver.

ACCESSION for	
NTIS	White Section <input checked="" type="checkbox"/>
DDC	Buff Section <input type="checkbox"/>
UNANNOUNCED	<input type="checkbox"/>
DESCRIPTION	
DISPATCH AVAILABILITY CODES	
SPECIAL	
A	

PRECEDING PAGE BLANK

CONTENTS

ABSTRACT	iii
I. INTRODUCTION	1
II. ANALYSIS	2
A. Monopulse Pattern	2
B. Signal-to-Noise Ratio	7
C. Two Way Antenna Patterns	9
III. CALCULATIONS	11
A. Test Example	11
B. Cases Considered	14
C. Airy Pattern LO	18
D. Gaussian Pattern	30
E. Uniform LO Distribution	40
F. Large Angle Search	47
IV. EFFECT OF TURBULENCE	53
V. CONCLUSIONS	54
ACKNOWLEDGMENT	54
REFERENCES	55
APPENDIX A	56

I. INTRODUCTION

Angle error signals can be obtained from a heterodyne detector which is broken up into four segments as depicted in Figure 1. If the local oscillator (LO) signal is symmetric on the detector and the received signal is centered on the detector, then there is an equal response from each quad element. As the target moves in angle, the receive beam moves on the detector and the output of each quad element changes. These signals can be used in an amplitude comparison monopulse system to obtain information about the angle of the target.

The monopulse error curves in a heterodyne detector system are a function of both the LO and received field distribution on the quad detector. These distributions are intimately involved with the consideration of the signal-to-noise, the total signal out of the detector, beamwidth, tracking error, and also have an effect on the sidelobe performance of the system.

In this note, expressions are derived and evaluated which allow one to determine the azimuth monopulse signal for various elevation cuts, the signal-to-noise out, efficiency, total signal out, and two way antenna patterns. The receive beam is considered to be an Airy pattern of arbitrary size on the detector. This corresponds to a uniform illumination in the input aperture and agrees closely with reality. The LO distributions considered at the detector are constant intensity and various size Gaussian and Airy patterns.

This analysis allows us to pick the optimum pattern to satisfy various criteria. The ramifications of the analysis on a multi element detector with a wide field-of-view are considered.

Turbulence is neglected in the analysis. A discussion of its effect on the patterns is included later.

II. ANALYSIS

A. Monopulse Pattern

Impinging on the detector which is shown in Figure 1 are the superimposed fields of the signal, $E_s(\bar{r})$, and the local oscillator, $E_o(\bar{r})$ which are functions of the position \bar{r} . The overbar indicates a vector quantity. It is assumed that the two fields have the same polarization so that the vector nature of the fields can be suppressed.

The two fields are represented in real form as

$$E_o = A_o(\bar{r}) \cos(\omega t + \phi_o(\bar{r})) \quad (1)$$

and

$$E_s = A_s(\bar{r}, \theta) \cos(\omega_s t + \phi_s(\bar{r})) \quad (2)$$

In general, the receive beam field is a function of the target angle, θ , with respect to boresight. The differential current induced by these fields from a small area of the detector is proportional to the total incident power, i.e.,

18-5-9452

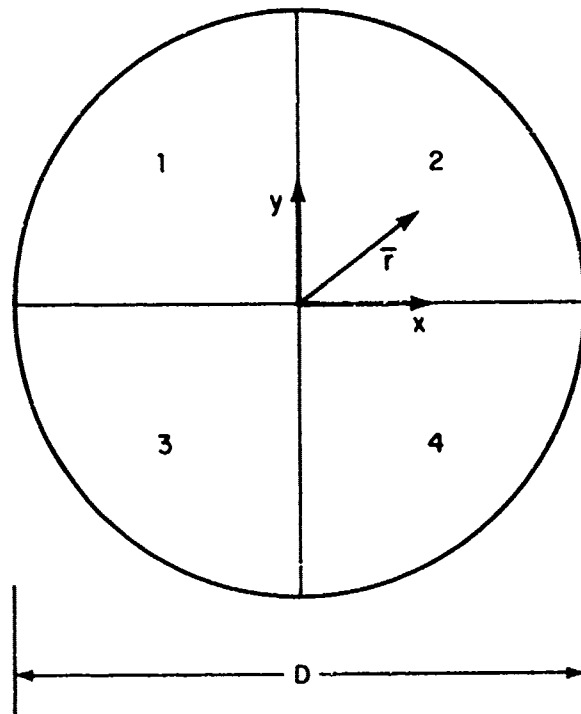


Fig. 1. Detector geometry.

$$di = \frac{n}{Z_0} (E_0 + E_s)^2 dA \quad (3)$$

where

$$n = eQ/hv$$

n relates the power incident on the detector to the current generated. Z_0 is the impedance of free space. Q is the number of electron hole pairs created for each quanta of energy.

The output of the detector occurs at DC and at the difference frequency. The DC term causes shot noise. The signal bearing term is

$$di' = \frac{n}{Z_0} A_0(\vec{r}) A_s(\vec{r}, \theta) \cos(\Delta\omega t + \Delta\phi(\vec{r})) dA \quad (4)$$

where

$$\Delta\omega = \omega_0 - \omega_s \quad (5)$$

and

$$\Delta\phi(\vec{r}) = \phi_0(\vec{r}) - \phi_s(\vec{r}) \quad (6)$$

The total signal current out of any quadrant, I_α , is found by integrating the differential current over its surface. Assuming uniform efficiency of electron-hole generation over the surface of the detector, one obtains,

$$I_{\alpha} = \frac{n}{Z_0} \int_{\alpha} A_0(\bar{r}) A_S(\bar{r}, \theta) \cos(\Delta\omega t + \Delta\phi(\bar{r})) dA \quad (7)$$

The sum channel current, I_S , is the sum of the currents in all four channels. The voltage out, V_S , is the current multiplied by the impedance of the channel, Z , and the gain of the channel G

$$V_S = I_S Z G_S \quad (8)$$

where

$$I_S = I_1 + I_2 + I_3 + I_4 = \frac{n}{Z_0} \left[\int_1 + \int_2 + \int_3 + \int_4 \right] \\ \times A_0(r) A_S(r, \theta) \cos(\Delta\omega t + \Delta\phi(r)) dA \quad (9)$$

and the electrical phase shifts have been considered to be the same in all four channels.

The azimuth channel voltage is

$$V_{Az} = I_{Az} Z G_{Az} \quad (10)$$

where

$$I_{Az} = I_2 + I_4 - I_1 - I_3 \quad (11)$$

and the elevation channel voltage is

$$V_{E1} = I_{E1} Z G_{E1} \quad (12)$$

where

$$I_{E1} = I_1 + I_2 - I_3 - I_4 \quad (13)$$

Let us discuss the phase term. If the LO and received signal phase front are parallel, then the output phase from each differential surface element is the same. This is true even if the detector surface is rough as long as the roughness is less than a wavelength at the difference frequency. As the receive beam is moved off axis, at first one might expect the two wavefronts to become tilted with respect to each other, but actually, as shown in the Appendix, if the limiting aperture is in the focal plane of a lens in the receive path, then the receive beam wavefront at the detector does not change tilt as the beam is moved off axis. Even if this condition is not satisfied exactly, the wavefront tilt near the optic axis for typical configurations is small and is negligible. For these reasons, the phase difference is considered to be constant.

With this preamble as a basis, the normalized azimuth mono-pulse signal, ΔAz , which is a ratio of the voltage in the azimuth channel to that in the sum channel can be written as

$$\Delta Az = \frac{V_{Az}}{V_s} = \frac{G_{Az} I_{Az}}{G_s I_s} = \frac{G_{Az}}{G_s} \frac{\left[\int_2 + \int_4 - \int_1 - \int_3 \right] A_o(r) A_s(r, \theta) dA}{\left[\int_1 + \int_2 + \int_3 + \int_4 \right] A_o(r) A_s(r, \theta) dA} \quad (14)$$

And similarly, the normalized elevation monopulse signal, $\Delta E1$, can be written as

$$\Delta E1 = \frac{V_{E1}}{V_s} = \frac{G_{E1} I_{E1}}{G_s I_s} = \frac{G_{E1}}{G_s} \frac{\left[\int_1 + \int_2 - \int_3 - \int_4 \right] A_o(\bar{r}) A_s(\bar{r}, \theta) dA}{\left[\int_1 + \int_2 + \int_3 + \int_4 \right] A_o(\bar{r}) A_s(\bar{r}, \theta) dA} \quad (15)$$

B. Signal-to-Noise Ratio

An expression for the sum signal has been developed and is given in Equation 9. The noise in the system will now be found. The noise current per square root of unit bandwidth due to the shot noise effect is given by

$$i_n = (2i_{av}e)^{1/2} \quad (16)$$

where e is the charge on an electron, and i_{av} is the average current flowing in the detector. Since the LO power is much larger than the signal power, it predominates in determining the average current. The average differential current, $\underline{d_i}$, can be found from Equation 3 as

$$\underline{d_i} = \frac{n}{2Z_o} A_o^2(\bar{r}) dA \quad (17)$$

The total average current can be found to be

$$i_{av} = \frac{n}{2Z_o} \left[\int_1 + \int_2 + \int_3 + \int_4 \right] A_o^2(\bar{r}) dA \quad (18)$$

The signal-to-noise ratio is equal to the average of the sum current squared divided by the noise current per square root of bandwidth squared, times the bandwidth, B.

$$\frac{S}{N} = \frac{I_s^2}{i_n^2 B} = \frac{n}{2Z_0 eB} \left(\frac{[\int A_0(\bar{r}) A_s(\bar{r}, \theta) dA]^2}{\int A_0^2(\bar{r}) dA} \right) \quad (19)$$

where the integrals are over the entire detector, and the underbar indicates a time average.

Since the total average signal power incident on the detector is

$$P_s = \frac{1}{2Z_0} \int A_s^2(\bar{r}, \theta) dA \quad (20)$$

then Equation 19 can be rewritten as

$$\frac{S}{N} = \frac{nP_s}{eB} \left\{ \frac{[\int A_0(\bar{r}) A_s(\bar{r}, \theta) dA]^2}{\int A_s^2(\bar{r}, \theta) dA \int A_0^2(\bar{r}) dA} \right\} \quad (21)$$

Note that for a given LO distribution, the noise power is constant and the expression for S/N is proportional to the receive beam pattern.

The last term in curly brackets is called the mixing efficiency and is a measure of the similarity of the LO and receive beam field pattern. By the use of the Schwartz inequality, it can be shown that the maximum of the expression is one and that

only occurs when the local oscillator field is proportional to the received field. As the received angle is moved off boresight, the patterns do not match as well and the term in curly brackets decreases. This along with the fact that less of the received power falls on the detector produces the receive beam pattern.

The mixing efficiency will be calculated for various beam distributions and even more importantly so will the expression for S/N given in Equation 19. One can have a very high mixing efficiency but a very low signal-to-noise ratio because only a small fraction of the received power falls on the detector as for instance, if the Airy disc of the receive beam is much larger than the detector. This will be discussed in more detail later.

The signal-to-noise ratio out of the detector is equal to that at the output of the system provided that the added noise due to the receive components is much less than the noise power out of the detector. In theory at least, this condition can be achieved because the noise power out of the detector can be increased with no change in S/N by increasing the LO power.

C. Two Way Antenna Patterns

The two way pattern of the system is useful in determining the two way loss, beamwidth, and the sidelobe levels. Since no beam shaping (apodization) is currently employed in the system, the sidelobe patterns are considerably higher than in a microwave radar. The receive beam pattern has already been determined. The transmit pattern will be discussed.

In general, the transmit and receive beamwidths can be arbitrary. For efficiency and the convenience of using the same transmit aperture, the two beamwidths are normally equal and it is this case we will consider.

First let us discuss a convention about beamwidth which is pertinent to the plots. The angular distance to the zeroes of an Airy pattern produced by a uniform illumination of the transmit aperture of diameter D is $2.44 \lambda/D$. The angular distance to the 3 dB points of the transmit pattern is about half this value which is $1.22 \lambda/D$. It is this latter value which we will consider as the beamwidth (BW). This is consistent with the accepted value of 10 μ rad beamwidth for the 48 inch aperture at Firepond.

The transmit beam is generally not uniform in intensity across the aperture. However, since the far field pattern is not too sensitive to the exact distribution, it will be considered constant in this analysis. The far field power pattern of a uniformly illuminated aperture is given by¹

$$T = [2J_1(7.664 \theta/BW)/(7.664 \theta/BW)]^2 \quad (22)$$

where θ is the angle off axis and J_1 is a Bessel function.

The dependence on range has been omitted since we are interested in the patterns at constant range.

The two way pattern, PAT, can now be found by taking the transmit field at any angle and multiplying it by the receive pattern at that same angle

$$\text{PAT} = T \times S \quad (23)$$

This is normalized in the plots to give unity on boresight.

III. CALCULATIONS

The various expressions involving integrals have been calculated numerically. The integral over each quadrant was found by breaking up the x and y coordinates into 20 segments, calculating the value in the center of each square and then summing up the contributions of the squares that fall upon the detector.

A. Test Example

As a check on the accuracy of the computer program and to illustrate in a more concrete fashion the results of the mono-pulse calculation, a problem which can be solved exactly is considered.

Let the LO beam be uniform over the detector and the receive beam be uniform in amplitude over a circle equal to the detector size whose diameter is D and zero outside this region. As the incoming angle of the received beam is changed, the area of overlap between the two beams changes. Figure 2 is an illustration of the situation when the two beams are separated by a

18-5-9453

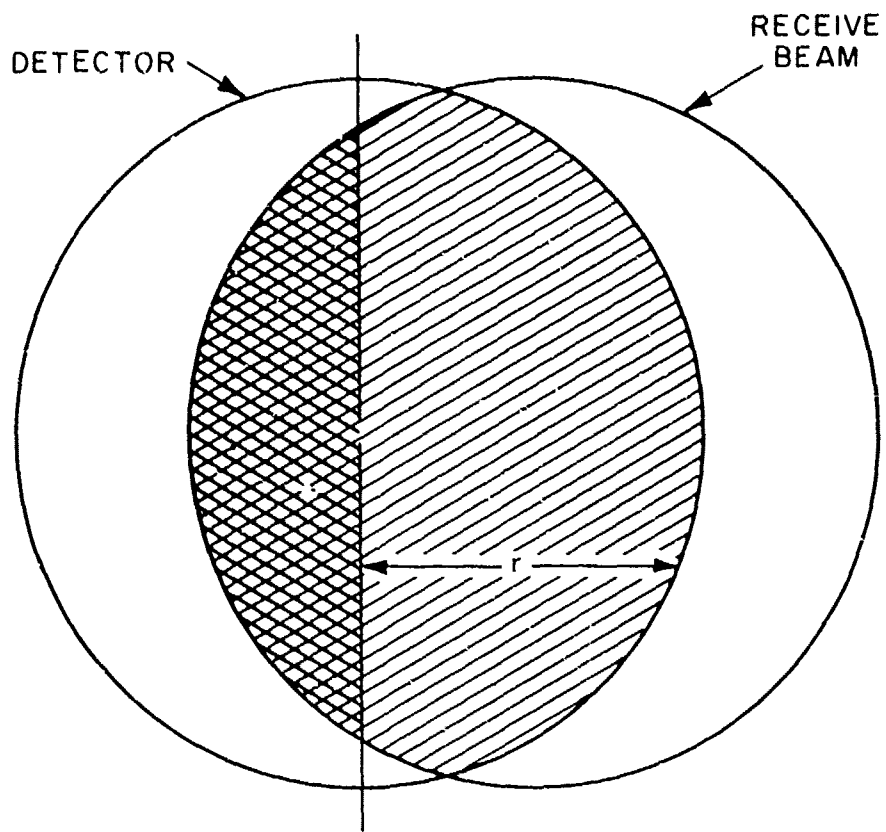


Fig. 2. Overlap of receive beam and detector.

distance r . It is easy to show that the area of overlap which is represented by the hatched area is

$$\begin{aligned} \text{Sum} &= \frac{1}{2} [D^2 \cos^{-1}(r/D) - r(D^2 - r^2)^{1/2}] \quad r \leq D \\ &= 0 \quad r > D \end{aligned} \quad (24)$$

The portion of overlap which is on the left hand side of the detector and is represented by the doubly hatched region is easily found to be

$$\begin{aligned} \text{Left} &= \frac{1}{2} \left[\frac{D^2}{2} \cos^{-1}(2r/D) - r(D^2 - 4r^2)^{1/2} \right] \quad r < D/2 \\ &= 0 \quad r > D/2 \end{aligned} \quad (25)$$

Obviously, the overlap on the right side is

$$\text{Right} = \text{Sum} - \text{Left}$$

The monopulse characteristics, therefore, is

$$\Delta Az = \frac{\text{Right} - \text{Left}}{\text{Sum}} = \frac{\text{Sum} - 2 \times \text{Left}}{\text{Sum}} \quad (26)$$

$$\begin{aligned} &= 1 - \frac{2[D^2/2 \cos^{-1}(2r/D) - r(D^2 - 4r^2)^{1/2}]}{D^2 \cos^{-1}(r/D) - r(D^2 - r^2)^{1/2}} \quad r \leq D/2 \\ &= 1 \quad D/2 < r < D \end{aligned} \quad (27)$$

This quantity has been calculated and compared to the computer results which were calculated and the agreement was with 3% for 25 beam positions.

Figure 3 illustrates the monopulse pattern for this case. The monopulse error increases steadily as the receive beam is moved in a radial direction. When the movement is one radius, none of the receive beam falls on the left hand side of the detector and the normalized monopulse error is now unity. This value persists until the receive beam falls completely off the detector at two beam radii.

The pattern is antisymmetric with only one half of the pattern shown. Notice that the pattern is not linear out to one radii offset. There is no reason to feel that the pattern should be linear.

B. Cases Considered

The receive beam is considered to be an Airy pattern at the detector for the remaining cases. In actuality, the true pattern deviates a little from this due to the structure holding the secondary and the obscuration of the secondary.

The effect of a small secondary such as the 8-inch secondary at Firepond is easily calculated by using superposition. In that case, the field at the aperture can be considered to be due to a uniform field over the 48-inch aperture and the negative of that field over the 8-inch aperture. The focused spot of the 8-inch beam is 6 times larger in diameter than the field of the 48-inch

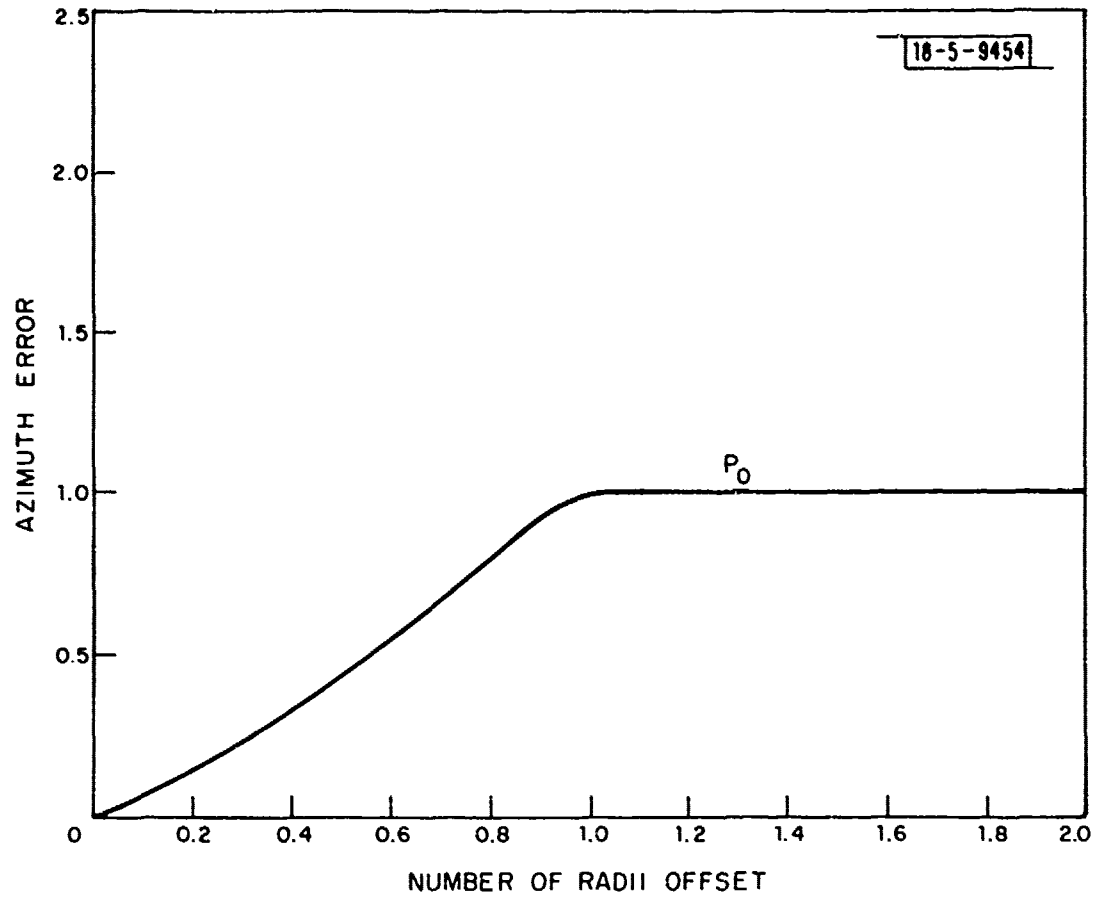


Fig. 3. Monopulse pattern for constant intensity L_0 and receive beam at aperture.

beam. The field on the detector due to the 8-inch beam is only 1/36 of the 48-inch beam. As the receive angle changes, the field due to the 8-inch beam changes very little because it corresponds to a larger beamwidth. Therefore, the obscuration essentially subtracts a constant power at the detector.

The effect of the secondary on the signal-to-noise ratio on axis has been considered for uniform and Gaussian LO distributions. by Klein and Degnan.² For small obscuration ratios, the results agree with those presented here.

The secondary support structure can have a greater effect because of its larger size. In actuality, because it obscures so little energy, it only adds a small astigmatism term at the detector. This is neglected.

With the above assumptions, the expression for the received field at the detector is

$$A_s(\bar{r}, \theta) = J_1(3.832r/R_r)/r \quad (28)$$

where

$$r = [(x - \theta_{Az}R_r/2BW)^2 + (y - \theta_{El}R_r/2BW)^2]^{1/2} \quad (29)$$

θ_{Az} and θ_{El} are the angular offsets of the receive signal from boresight in the azimuth and elevation directions respectively, and R_r is equal to the receive beam size at the detector. When

R_r equals the detector radius, the zeroes of the receive beam fall at the detector edge.

The fields for the three LO distributions that are considered are:

- 1) For the constant field case

$$A_o(\bar{r}) = 1 \quad (30)$$

- 2) For the Gaussian LO case

$$A_o(\bar{r}) = 1/\omega \exp[-(r/\omega)^2] \quad (31)$$

where ω is proportional to the beam size.

- 3) For the Airy pattern LO case

$$A_o(\bar{r}) = \frac{J_1(3.832r/R_1)}{r} \quad (32)$$

where R_1 is equal to the LO size on the detector and r is the distance from the center of the detector.

The reason these fields are chosen is that they are easy to achieve experimentally. Lasers normally put out a spatial pattern which is Gaussian. If this field is combined with the receive beam and then focused on the detector, the resulting LO field is also Gaussian. In actuality, the Gaussian field is truncated by the laser and focusing lenses; however, for lenses as large as

several times the $1/e^2$ point of the field distribution, the assumption of a Gaussian distribution is a good approximation.

The Airy pattern distribution on the detector can be closely achieved by using just the central part of the LO Gaussian beam distribution which is fairly uniform in intensity. If this central spot is expanded to the size of the final lens, then the focused field of this fairly uniform intensity distribution is an Airy pattern on the detector.

If, however, the final size of the uniform intensity distribution is small compared to the size of the final focusing lens, then the focused LO distribution is an Airy pattern whose size is much larger than the detector. This is a good approximation of a uniform intensity distribution on the detector.

C. Airy Pattern LO

The size of the LO Airy disc on the detector can be increased by decreasing the spot size of the LO on the focusing lens. Since the receive beam pattern is also Airy on the detector, one can obtain an exact match of beam patterns if the LO and receive beam are the same size on the final lens.

Figure 4 gives the monopulse error plots for an LO pattern with zeroes at the edge of the detector and various size receive beam patterns. Zeroes of the receive beam are at .5, .67, .8, 1.0, 1.3 and 2.0 times the detector size. There are several interesting things to be noted. First, the slope of the monopulse curve is not constant and, in fact, differs by a factor of

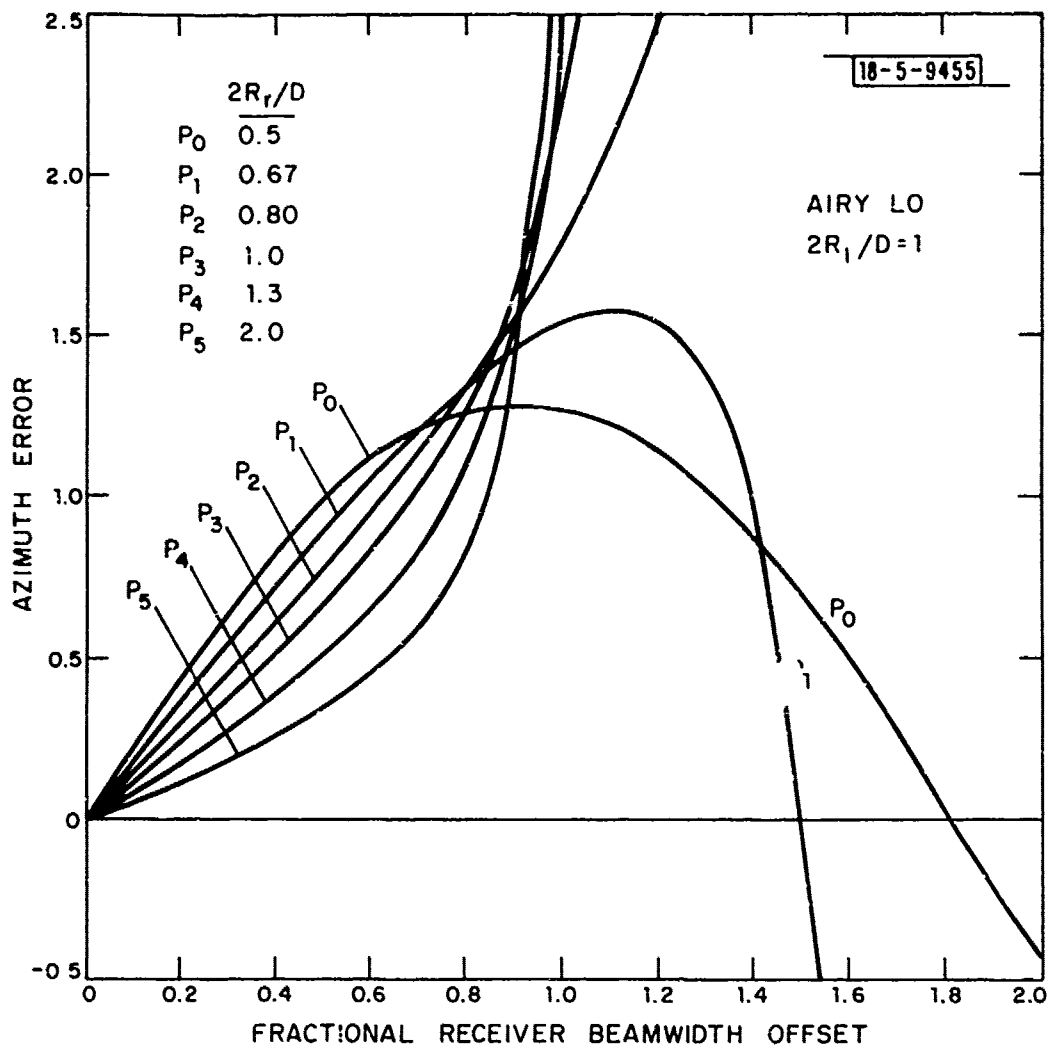


Fig. 4. Normalized monopulse pattern for Airy LO pattern whose zeros fall at the edge of the detector and various receive beam sizes. Receive beam zeros are at .5, .67, .80, 1.0, 1.3 and 2 times the detector radius.

4 as the receive beam size changes by a factor of 4. The curves go negative for large offsets due to the sidelobes of the Airy function. The monopulse pattern stays positive longer when the receive beam size is less than the detector size.

Although the graphs don't illustrate it, the monopulse pattern actually goes to infinity because the sum pattern goes to zero for some angular offsets due to the Airy disc sidelobes. If the difference signal goes to zero before the sum signal as the off boresight angle is measured, then the more normal looking monopulse curves with negative second derivative result. However, if the sum signal goes to zero first, then the normalized monopulse error goes to infinity before it changes sign. The monopulse error can be greater than one because the negative contribution of the sidelobes can cause the sum signal to be less than the difference signal. The monopulse curves are suppressed on these and all subsequent curves after the error changes sign. This is done to make the plots less cluttered.

The monopulse curves do not change sign for an offset of at least a beamwidth. Therefore, the monopulse system can be used to track for offsets of at least ± 1 beamwidth.

Figure 5 illustrates the mixing efficiency. It is unity for the case where the two patterns are the same size. It is interesting to note that one can get an efficiency of .7 by overlapping the sidelobe of the receive beam pattern with the LO pattern in one case.

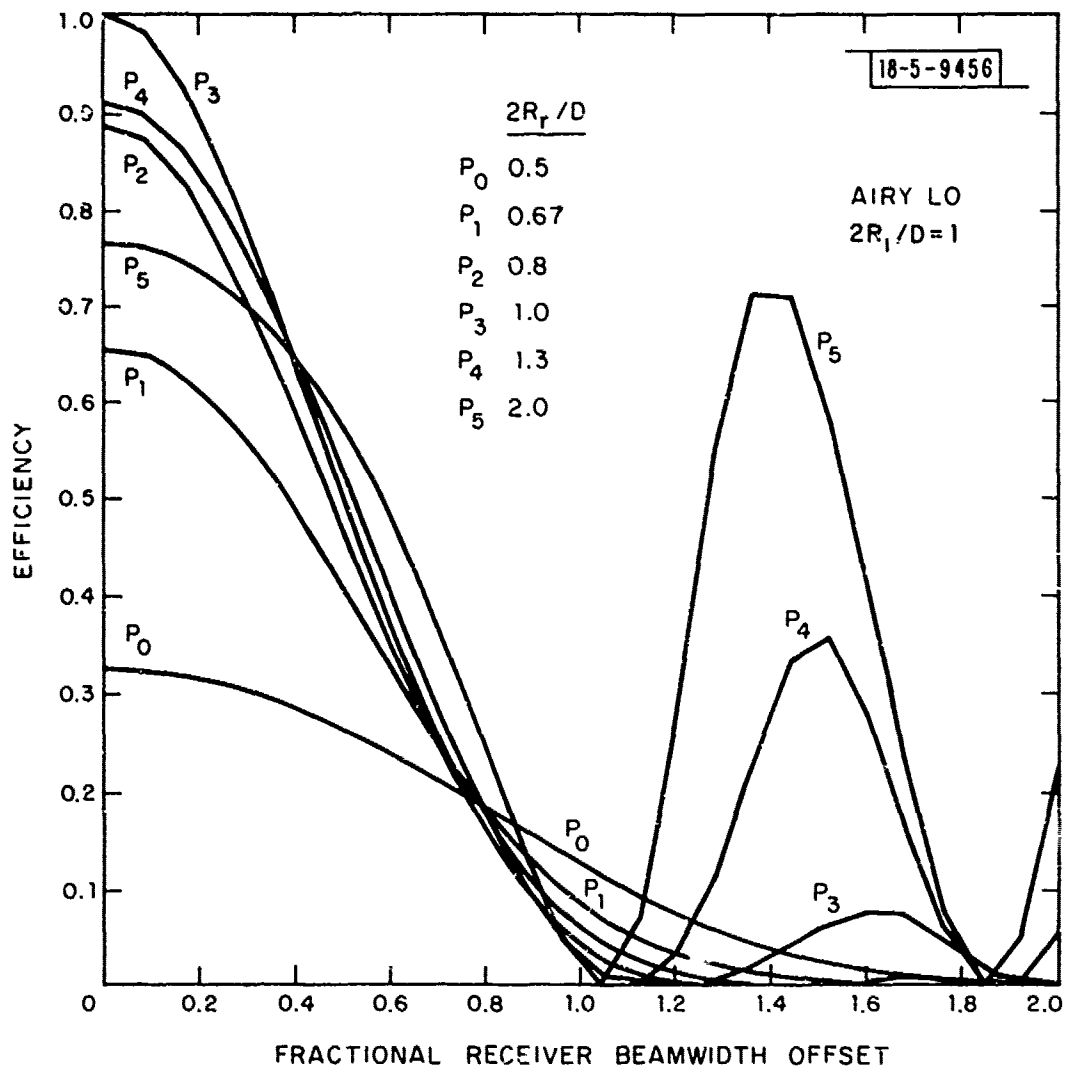


Fig. 5. Efficiency for beams described in Fig. 4.

Figure 6 illustrates the normalized signal-to-noise for the various cases. The normalization is such that the S/N would be one if all the receive beam energy fell on the detector and the LO pattern exactly matched it. The highest S/N occurs for the case of the receive beam exactly matching the LO beam. The value is .84 which corresponds to the energy in the first Airy disc. The efficiency can be increased by making both the LO and receive beam patterns smaller on the detector.

Figure 7 gives the two way pattern for the same receive beam sizes. These curves are normalized to unity on boresight. Notice that the pattern with the best signal-to-noise has a sidelobe level of 43 dB while the one with the most linear monopulse error curve has a sidelobe level of 26 dB. Also note that the 6 dB beamwidth varies by 20% for different cases.

From the output of many different cases, one can make a tabulation of the quantities which affect system performance. The characteristics of interest are:

1. $(S/N)_N$ - The on axis normalized S/N ratio. The maximum this can attain is 1.0 when all the receive energy falls on the detector and it exactly matches the LO distribution.
2. k_m - The on axis normalized monopulse slope. This is equal to the change in normalized monopulse error divided by the fraction beamwidth change in offset.

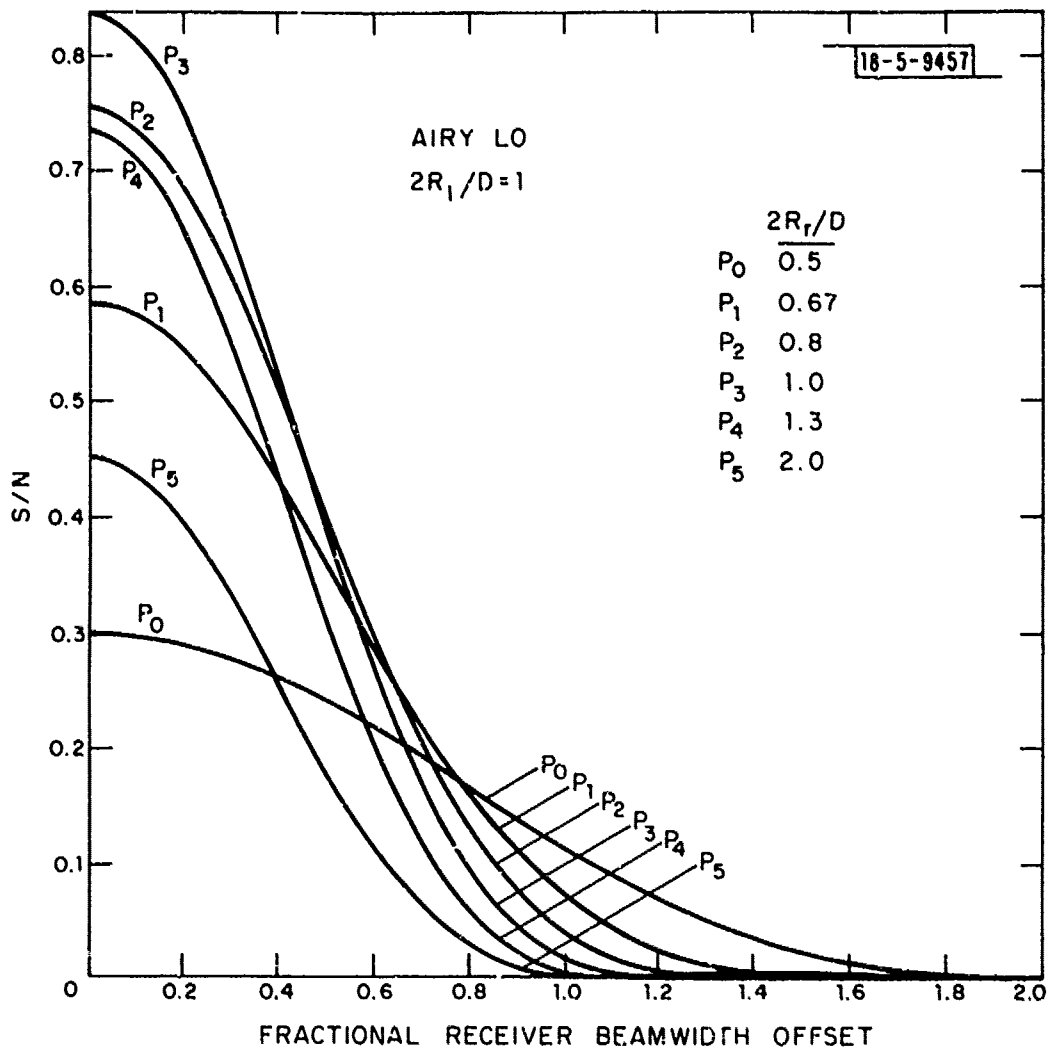


Fig. 6. Normalized signal-to-noise ratio for patterns described in Fig. 4.

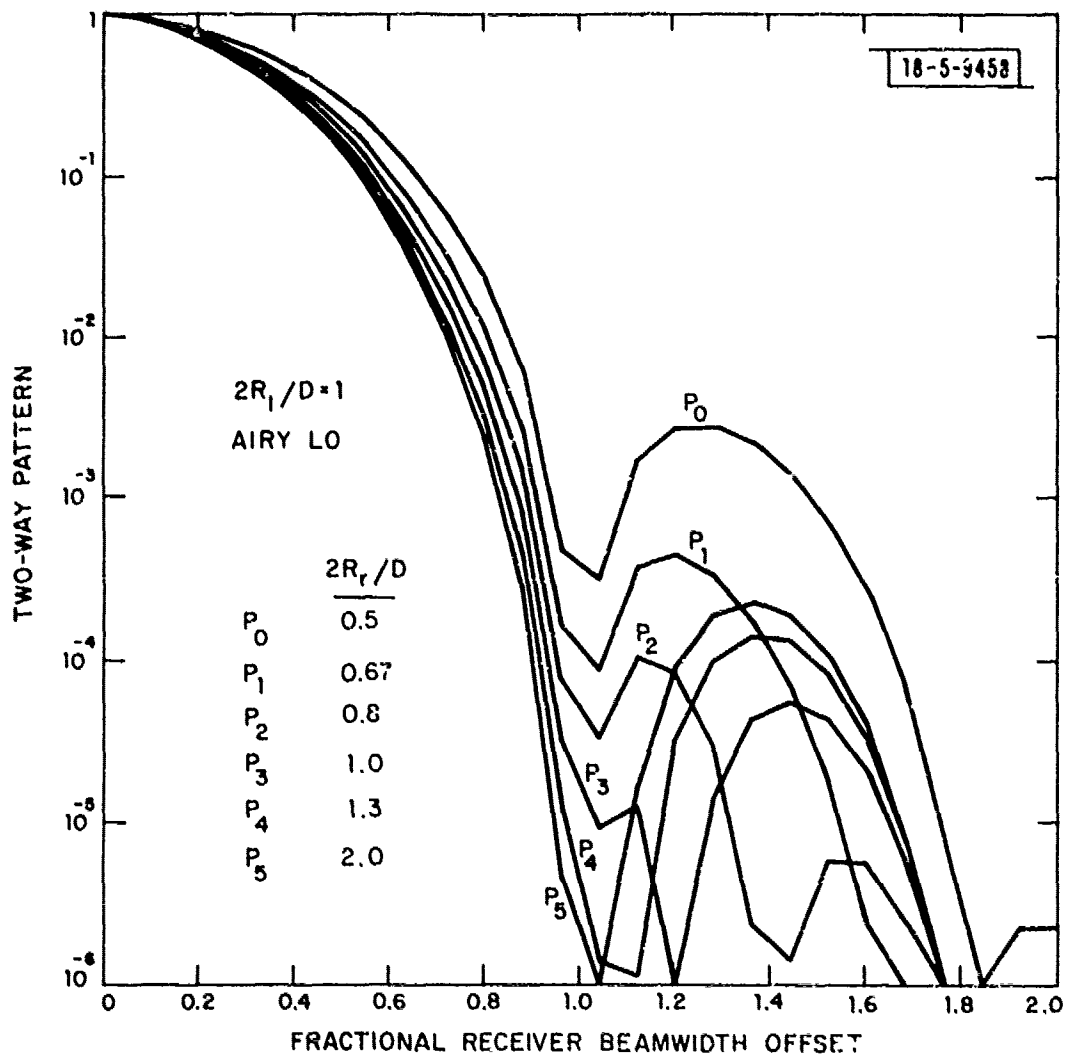


Fig. 7. Normalized two way pattern for beams described in Fig. 4.

The beamwidth, BW, is defined to be one-half the angle between the zeroes of the receive beam pattern.

3. $(\theta_{\text{RMS}})_N$ - The normalized on axis monopulse tracking error is defined to be

$$(\theta_{\text{RMS}})_N = \frac{\text{BW}}{k_m \sqrt{2(S/N)_N}} \quad (33)$$

The fractional beamwidth RMS angle tracking jitter can be found by dividing this number by the square root of the computed S/N assuming no mismatch loss on the detector.³

4. $(\theta_R)_{3\text{dB}}$ - The angle between the 3 dB points of the receive beam. This is the angle between the point at which the signal in the receive beam has dropped to one-half of its on axis value.
5. $(\theta_{\text{TW}})_{6\text{dB}}$ - The angle between the 6 dB points of the two way beam pattern. Assuming an Airy transmit pattern in the far field, this is the angle between the points at which the two way pattern has fallen by a factor of 4 from its on boresight value.
6. θ_s - The search beamwidth. This is defined to be the angle between the points at which the two way pattern is one quarter of the ideal value, i.e., assuming $(S/N)_N$ is unity. This is related to how far apart the angular beam patterns can be when one is performing an

angle search in which a 6 dB loss is allowed at the overlap points. Obviously, different criteria could be used and the results would differ.

7. $\theta(\text{Mono})_U$ - The angular extent of the curves on one side of boresight for which the monopulse curves are unambiguous.
8. $\theta(\text{Mono})_T$ - The angular extent of the curves on one side of boresight for which the monopulse curve is the correct sign even though it may be ambiguous. If there is an asterisk next to the number, it indicates that even though the sign of the sum signal changed sign within that interval, the difference signal also changed sign in less than .08 beamwidth. Therefore, the normalized monopulse signal is the correct sign for most of the interval.
9. SL(dB) - The level of the first sidelobe of the two way pattern with respect to the on boresight signal.

These quantities are listed for various LO and receive beam sizes in Table 1.

There is one case for which several parameters are optimized. Figure 8 and 9 depict the azimuth and elevation errors for elevation errors for elevation offsets of 0, .2, .4, .6, .8 and 1.0 BW for the case of the receive beam being two-thirds the detector size ($2R_r/D = .67$) and the zeros of the LO beam being four-fifths

TABLE I
 VARIATION OF PARAMETERS OF INTEREST FOR VARIOUS RECEIVE BEAM
 AND LO SIZES WITH AN AIRY LO DISTRIBUTION

$2R_T/D$	$2R_1/D$	$(S/N)_N$	k_m	$(\theta_{RMS})_N$	$(\theta_R)_{3dB}$	$(\theta_{TW})_{6dB}$	θ_s	$\theta(Mono)_N$	$\theta(Mono)_T$	SL(dB)
.50	1.33	.15	2.4	.76	2.60	1.10	---	.8	2.0	-22
.67	1.33	.33	2.4	.51	1.60	1.00	.48	.9	1.6	-27
.80	1.33	.55	2.0	.48	1.20	.96	.74	1.0	1.5	-33
1.00	1.33	.76	1.5	.54	.90	.92	.84	1.3	1.3	-42
1.33	1.33	.81	1.1	.71	.90	.88	.82	1.2	1.2	-41
2.00	1.33	.57	.7	1.30	.88	.88	.68	1.1	1.1	-37
.50	1.00	.30	2.3	.57	1.64	1.00	.36	.9	1.8	-26
.67	1.00	.58	1.9	.49	1.10	.96	.76	1.1	1.5	-34
.80	1.00	.76	1.5	.54	1.04	.94	.84	1.4	2.0*	-40
1.00	1.00	.84	1.2	.64	.94	.90	.76	1.2	1.2	-43
1.33	1.00	.73	.9	.92	.92	.88	.76	1.1	1.1	-38
2.00	1.00	.45	.6	1.80	.88	.88	.56	1.0	1.0	-36
.50	.80	.50	2.0	.50	1.28	1.00	.76	1.1	1.5	-32
.67	.80	.82	1.5	.52	.98	.90	.88	1.2	1.2	-46
.80	.80	.85	1.2	.64	.92	.88	.84	1.2	1.2	-40
1.00	.80	.74	.9	.91	.90	.88	.76	1.1	1.1	-37
1.33	.80	.52	.6	1.60	.86	.84	.62	1.0	1.0	-36
2.00	.80	.26	.4	3.50	.76	.76	.16	1.0	1.0	-35
.50	.67	.69	1.8	.49	1.06	.94	.82	1.3	1.3	-40
.67	.67	.89	1.1	.68	.88	.88	.84	1.1	1.1	-37
.80	.67	.78	.8	1.00	.86	.86	.76	1.0	1.6	-35
1.00	.67	.55	.7	1.40	.84	.76	.64	1.0	1.0	-35
1.33	.67	.30	.3	4.30	.76	.84	.32	1.0	1.0	-35
2.00	.67	.12	.13	16.30	.86	.84	---	1.0	1.0	-35
1.75	1.75	.91	1.1	.67	.87	.86	.84	1.1	1.1	-35
2.00	1.75	.85	1.5	.51	.95	.90	.84	1.2	1.2	-37
2.50	1.75	.56	2.0	.47	1.20	.96	.74	1.2	2.0*	-35
3.00	1.75	.36	2.1	.56	1.40	1.04	.56	1.0	1.7	-27
2.00	2.00	.91	1.1	.67	.88	.88	.84	1.1	1.1	-35
2.50	2.00	.75	1.6	.51	.90	.96	.83	1.2	1.2	-33
3.00	2.00	.49	2.0	.51	1.30	.94	.70	1.0	1.5	-38

*Sum and difference signals change sign within .08 BW.

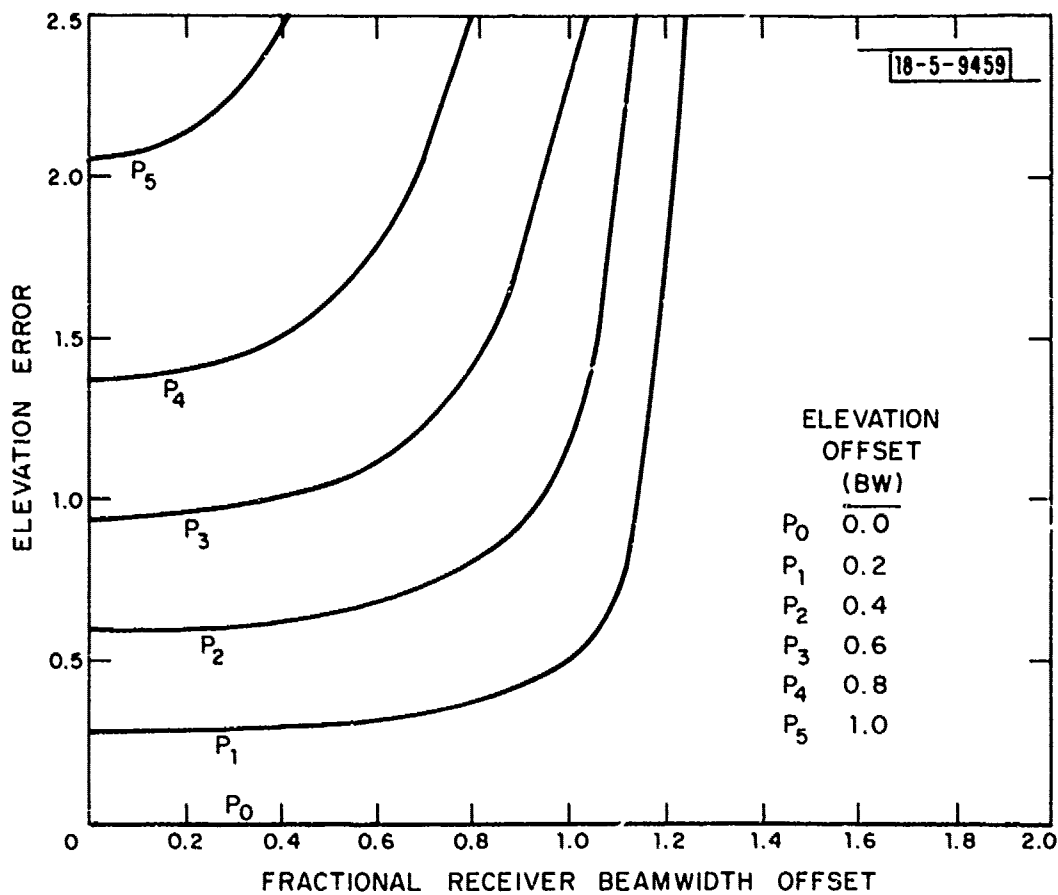


Fig. 8. Off axis normalized elevation curves for an Airy L0 which is .8 times the detector size and a receive beam which is .667 times the detector size.

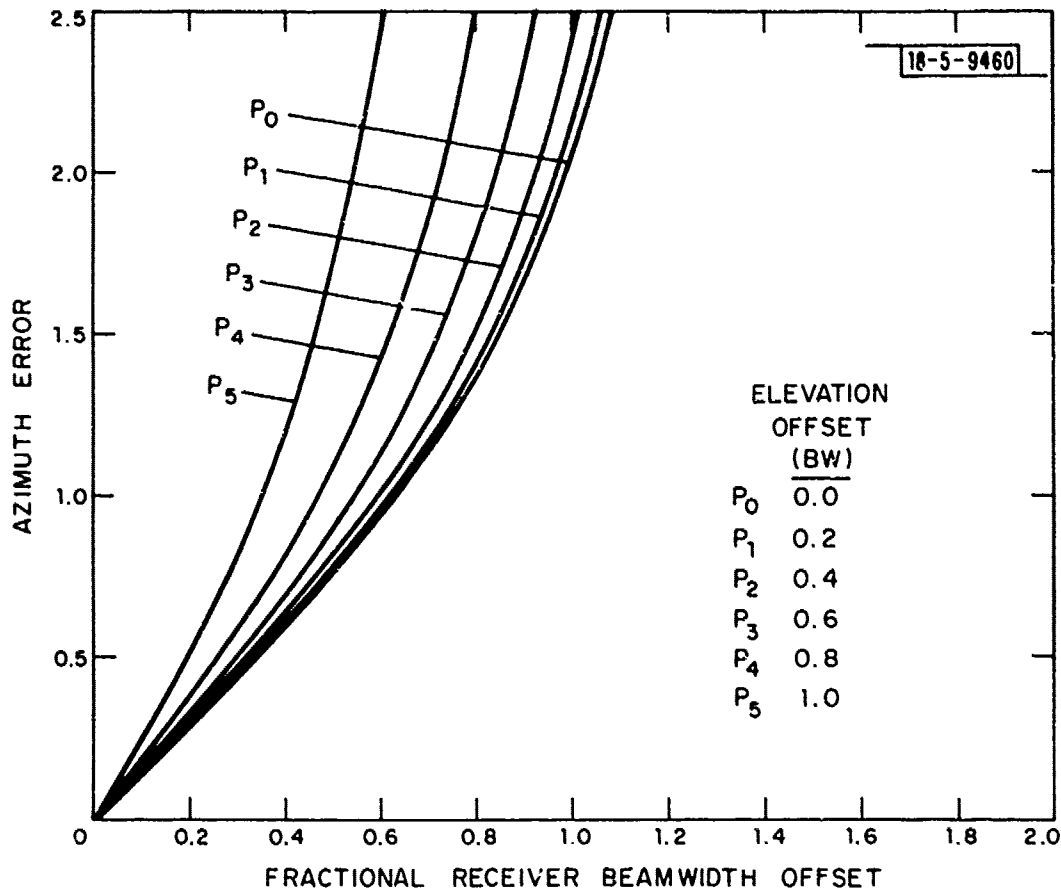


Fig. 9. Normalized azimuth error curves for the case described in Fig. 8.

the detector size ($2R_1/D = .80$). This case has an on axis $(S/N)_N$ of .82, a small tracking error of .52 and a first side-lobe level which is down 46 dB. Note the coupling between the azimuth and elevation curves.

There is a wide variation in the values of the parameters. Note that the best normalized on axis tracking errors correspond to a value of about .5. This means that with 20 dB S/N, the angle estimate would have an RMS error of one-twentieth of a beamwidth. A value of S/N of 28 dB is necessary to reduce the RMS angle error to a fiftieth of a beamwidth.

The receive beam angle can be seen to vary greatly in size and this will be explored when large angle search is considered later. The two way beam angular size does not vary greatly.

The extent of the unambiguous monopulse does vary a fair amount. There are choices of beam sizes which have the correct sign out to two beamwidths except for a region of less than .08 beamwidth during which both the sum and difference signals change sign to keep the normalized error the same sign.

The sidelobe level is seen to vary by over 20 dB for various receive beam sizes.

D. Gaussian Pattern

A Gaussian pattern LO with an Airy pattern receive beam is now considered. First a sampling of cases is presented which shows that the shape and characteristics are similar to those

of the Airy LO pattern. Then the characteristics for various beam sizes are tabulated.

Figure 10 gives the monopulse patterns for the case when the LO field is $\exp(-9/4)$ at the detector edge and the receive beam is the 6 sizes previously considered (.5, .67, .8, 1.0, 1.3 and 2.0 times the detector size). Notice that the curve marked P2 which corresponds to the receive beam size being .8 times the detector size is quite linear.

Figure 11 is the efficiency for these cases. Note that the efficiency can be close to unity for the case where the receive beam size is equal to the detector size. This is a consequence of the close match which is possible between an Airy and Gaussian function. This is illustrated in Figure 12.

Figure 13 gives the normalized S/N ratio for these cases. The curve corresponding to the most linear monopulse pattern has a value of .78. Figure 14 gives the two way pattern for this case. The case with the linear monopulse characteristic has a sidelobe level of 37 dB.

Figure 15 gives the azimuth error for elevation offsets up to a beamwidth for the linear monopulse characteristic. Figure 16 gives the elevation errors for this case.

Many different cases corresponding to various LO and receive beam sizes have been analyzed. A summary of the S/N ratio for these cases is picture in Figure 17. The normalized signal-to-ratio can be over .8 in the region in which the LO and receive

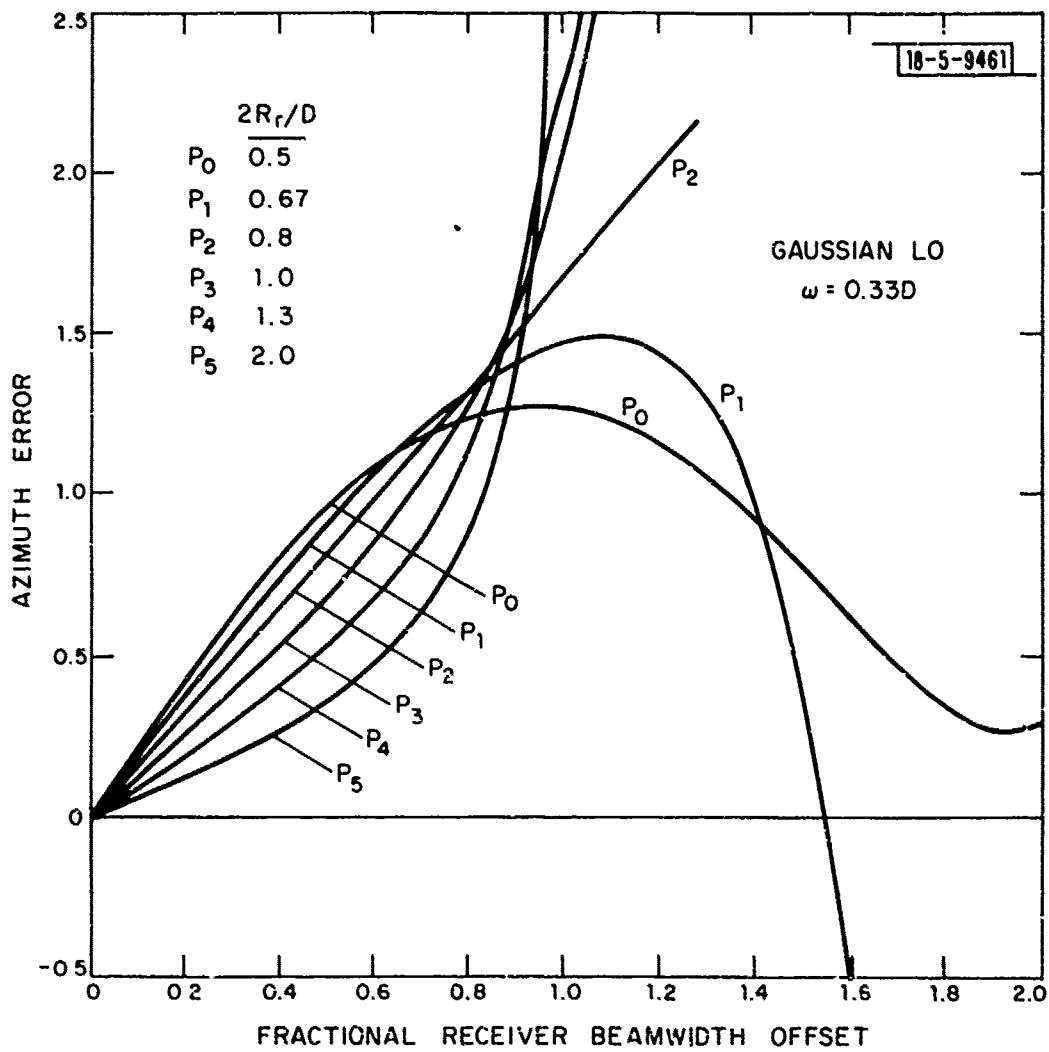


Fig. 10. Normalized azimuth errors for a Gaussian LO with various receive beam sizes.

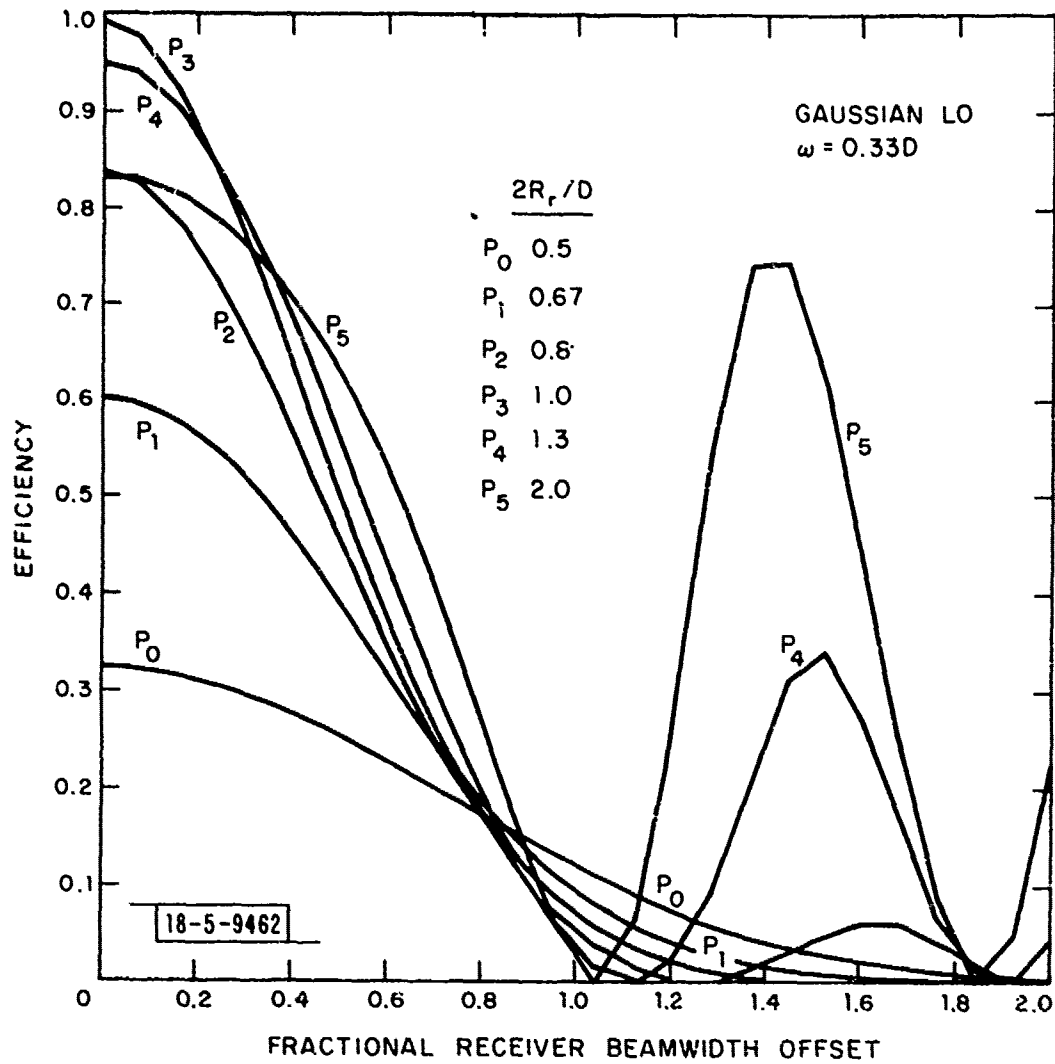


Fig. 11. Efficiency for case considered in Fig. 10.

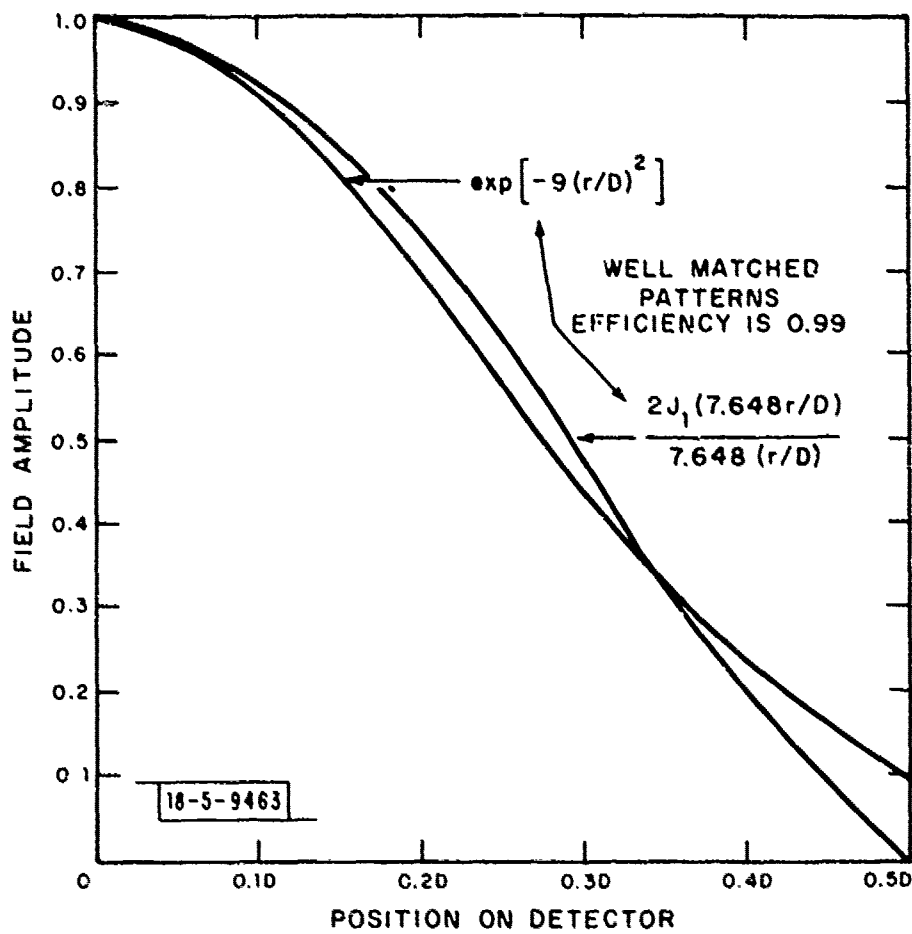


Fig. 12. Comparisons of Gaussian and Airy distributions on the detector.

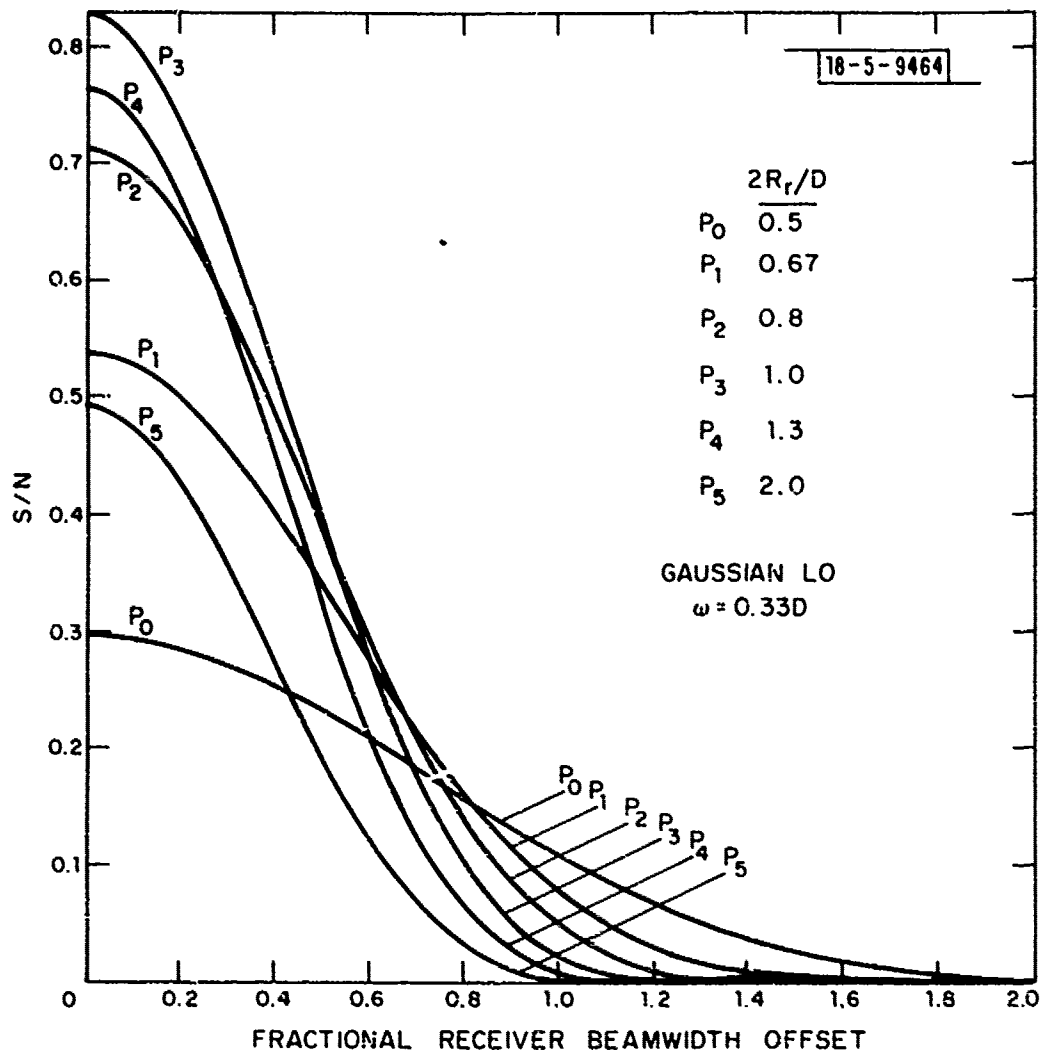


Fig. 13. Normalized signal-to-noise ratio for the case considered in Fig. 10.

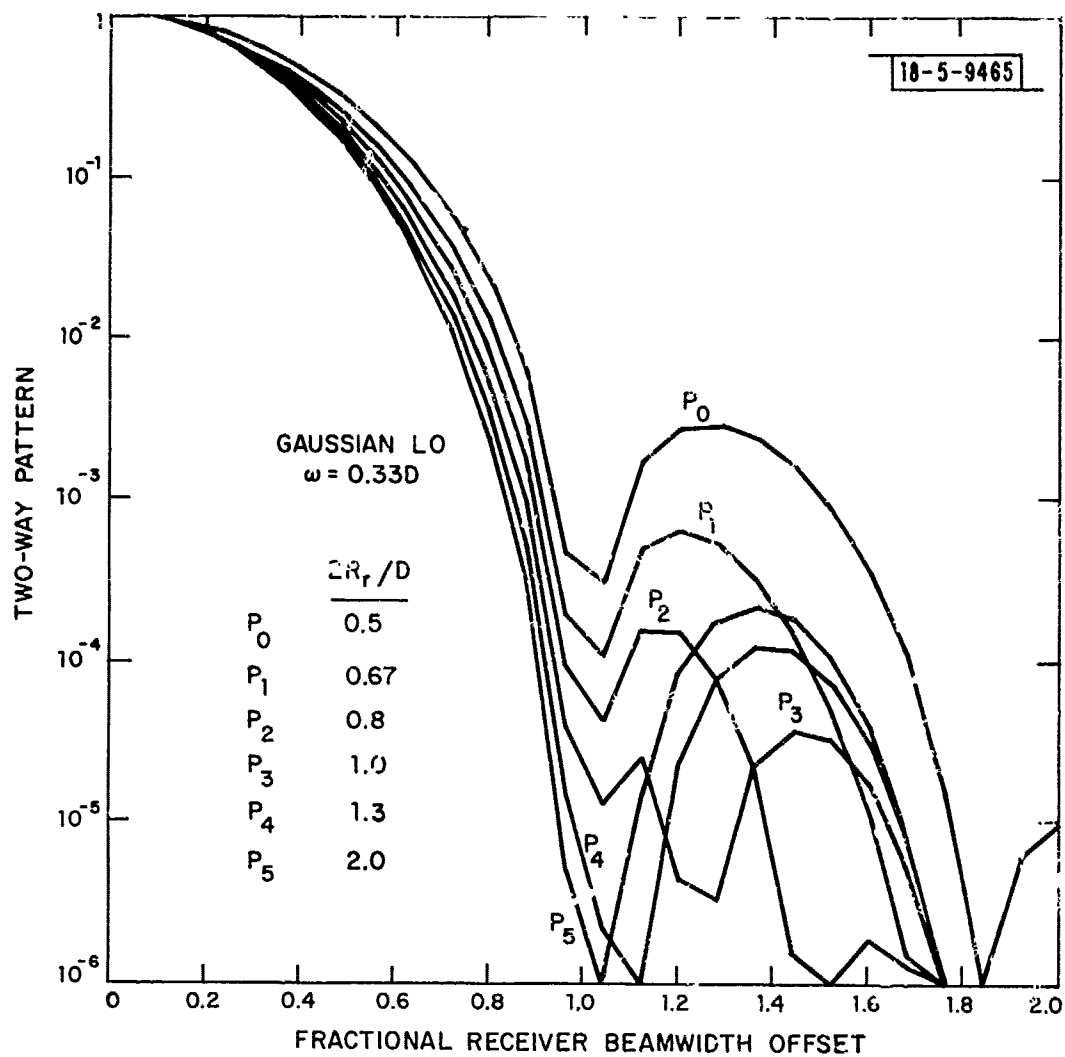


Fig. 14. Normalized two way pattern for the case considered in Fig. 10.

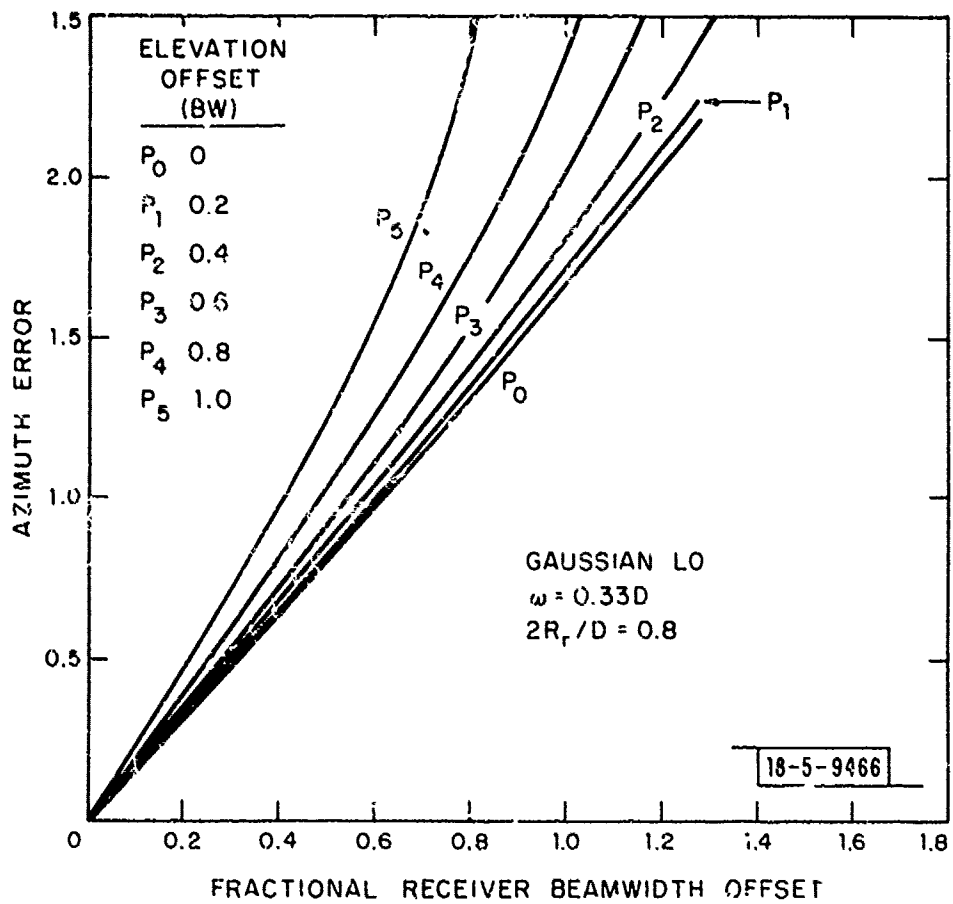


Fig. 15. Normalized azimuth error curves for various elevation offsets.

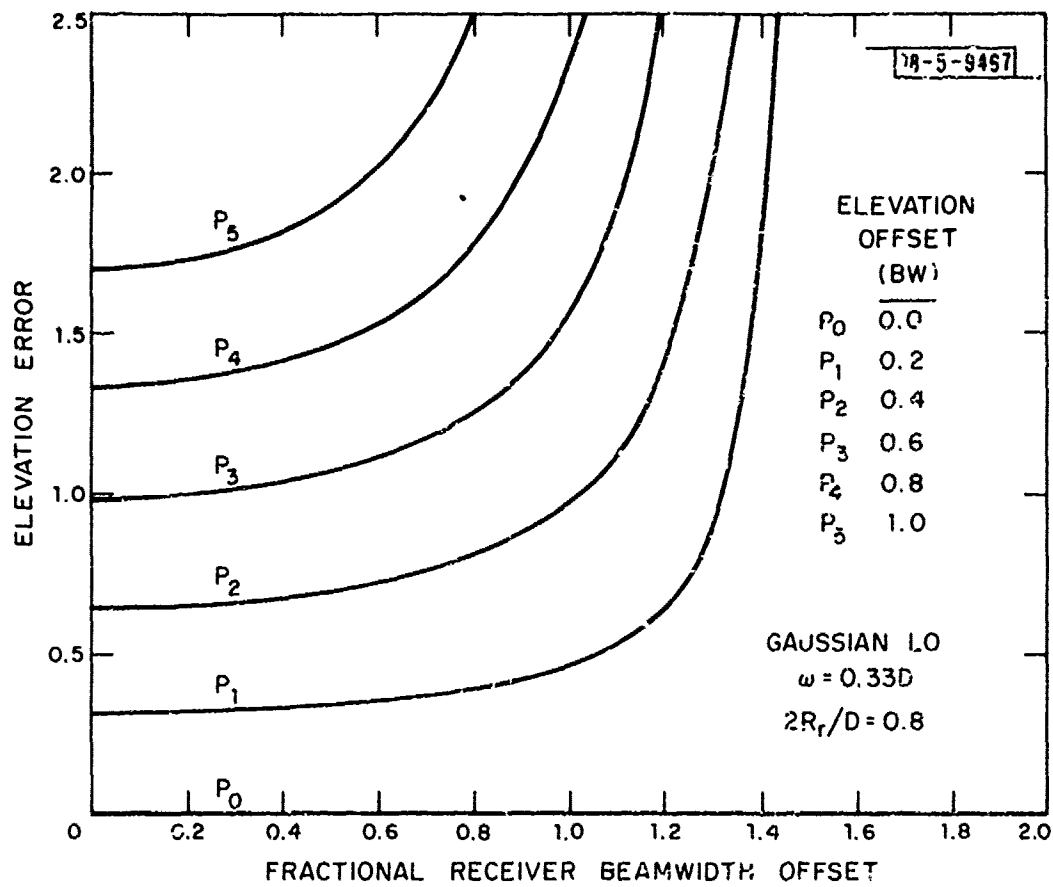


Fig. 16. Normalized elevation error curves for various elevation offsets.

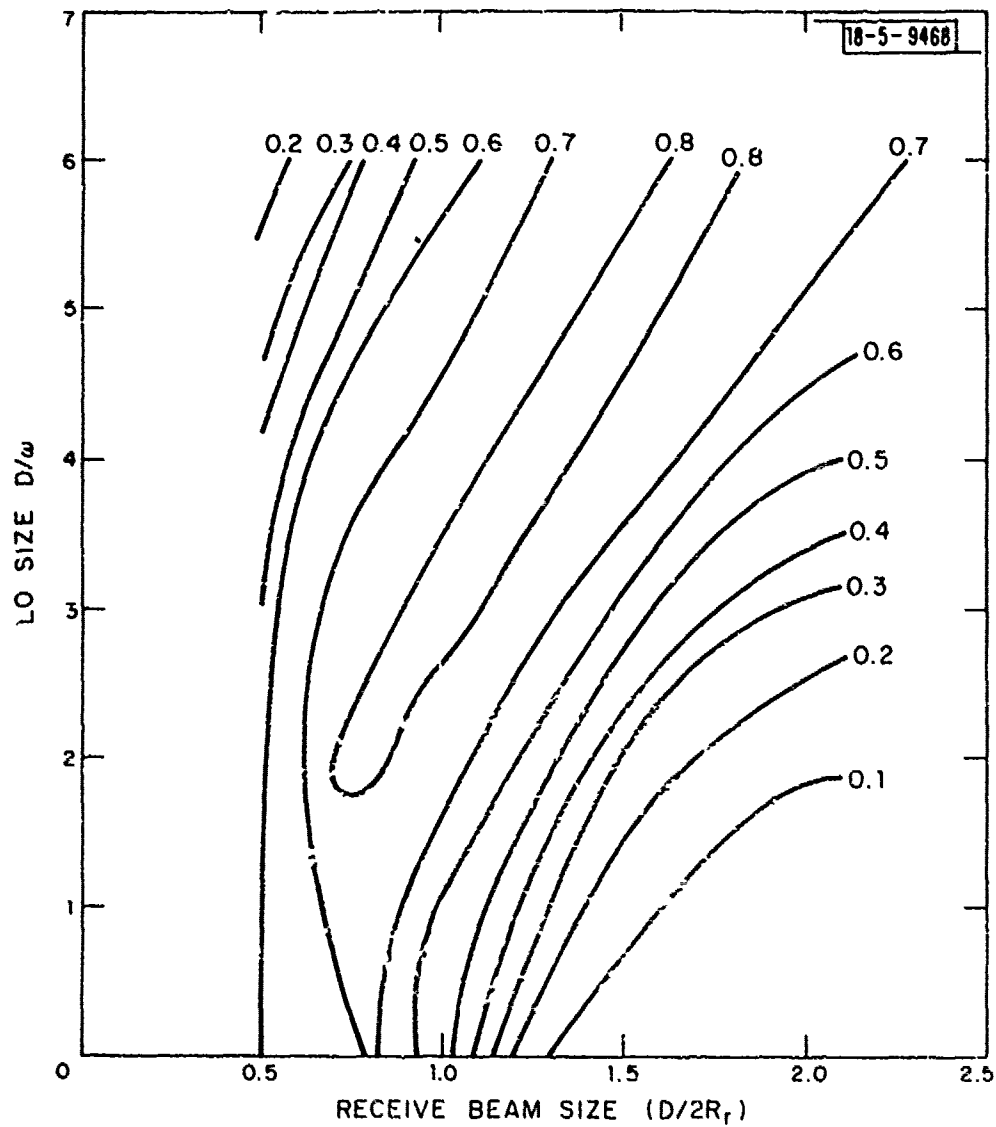


Fig. 17. Normalized signal-to-noise ratio for a Gaussian LO of various sizes vs the size of the receive beam.

patterns match which is approximately for ω equal to two-thirds R_r . The S/N falls off for large values of R_r because much of the receive beam energy does not fall on the detector.

The quantities of interest are tabulated in Table 2 for various LO and receive beam sizes. Note that the range of parameters' values is similar to that of the Airy LO.

E. Uniform LO Distribution

Next the case of a uniform LO with various receive beam sizes is considered. The quantities of interest are tabulated in Table 3. The normalized S/N has its peak around a receive beam size equal to the detector size. The on axis $(S/N)_N$ can be found exactly by integrating the term in parentheses in Equation 19 to give

$$\frac{S}{N} = \frac{1.04R_r^2}{D^2} \left[1 - J_0\left(\frac{1.916D}{R_r}\right) \right] \quad (34)$$

This and the sidelobe level are plotted versus beam size in Figure 18.

The monopulse error curves for the receive beam size being .9, 1.0, 1.11 and 2.0 times the detector diameter are depicted in Figure 19. Figure 20 shows $(S/N)_N$ for these cases and Figure 21 has the two way patterns.

The case in which the receive beam size is 1.11 times the detector size has reasonable $(S/N)_N$, low tracking error and low

TABLE 2
 VARIATION OF PARAMETERS OF INTEREST FOR VARIOUS RECEIVE BEAM
 AND LO SIZES WITH A GAUSSIAN LO DISTRIBUTION

$2R_r/D$	$2\omega/D$	$(S/N)_N$	K_m	$(\theta_{RMS})_N$	$(\theta_R)_{3dB}$	$(\theta_{TW})_{6dB}$	θ_s	$e(\text{Mono})_N$	$e(\text{Mono})_T$	SL(dB)
.50	.50	.13	2.4	.82	2.80	1.20	---	.8	2.0	-20
.67	.50	.29	2.5	.53	1.70	1.08	.36	.9	1.6	-26
.80	.50	.50	2.0	.50	1.24	.96	.70	1.0	1.5	-33
1.00	.50	.73	1.6	.52	1.04	.92	.82	1.4	2.0*	-40
1.33	.50	.80	1.4	.56	.92	.88	.82	1.2	1.2	-42
2.00	.50	.58	.7	1.30	.88	.88	.68	1.1	1.1	-37
.50	.35	.29	2.1	.62	1.60	1.04	.36	.9	2.0	-25
.67	.33	.54	1.9	.51	1.22	.96	.74	1.0	1.6	-33
.80	.33	.71	1.6	.52	1.06	.92	.82	1.3	2.0*	-38
1.00	.33	.83	1.2	.62	.96	.88	.86	1.2	1.3	-45
1.33	.33	.77	1.0	.85	.90	.88	.78	1.1	1.1	-38
2.00	.33	.49	.6	1.60	.86	.86	.60	1.1	1.1	-37
.50	.25	.51	1.9	.52	1.20	.94	.72	1.0	1.6	-32
.67	.25	.74	1.5	.55	1.04	.92	.84	1.5	2.0*	-39
.80	.25	.82	1.3	.62	.96	.88	.84	1.3	1.3	-46
1.00	.25	.79	1.0	.80	.90	.84	.80	1.2	1.2	-41
1.33	.25	.63	.8	1.10	.88	.88	.72	1.1	1.1	-37
2.00	.25	.36	.6	2.00	.88	.88	.46	1.0	1.0	-36

*Sum and difference signals change sign within .08 BW

TABLE 3
 VARIATION OF QUANTITIES OF INTEREST FOR VARIOUS RECEIVE BEAM
 SIZES WITH A UNIFORM LO DISTRIBUTION

$2R_T/D$	$(S/N)_N$	k_m	$(\theta_{RMS})_N$	$(\theta_R)_{3dB}$	$(\theta_{TW})_{6dB}$	θ_s	$\theta(\text{Mono})_N$	$\theta(\text{Mono})_T$	SL (dB)
.67	.10	3.50	.64	2.80	1.20	---	.7	1.9	-18
.80	.27	2.60	.52	1.80	1.10	.24	.6	1.6	-27
.90	.41	2.25	.49	1.30	.98	.60	1.0	1.5	-32
1.00	.53	1.90	.52	1.14	.96	.72	1.1	1.5	-36
1.11	.63	1.60	.55	1.02	.92	.76	1.4	2.0*	-39
1.33	.71	1.25	.64	.94	.90	.78	1.2	1.2	-44
1.50	.71	1.15	.73	.92	.88	.78	1.1	1.1	-42
2.00	.58	.83	1.12	.88	.86	.70	1.1	1.1	-37

*Sum and difference signal change sign within .08 BW.

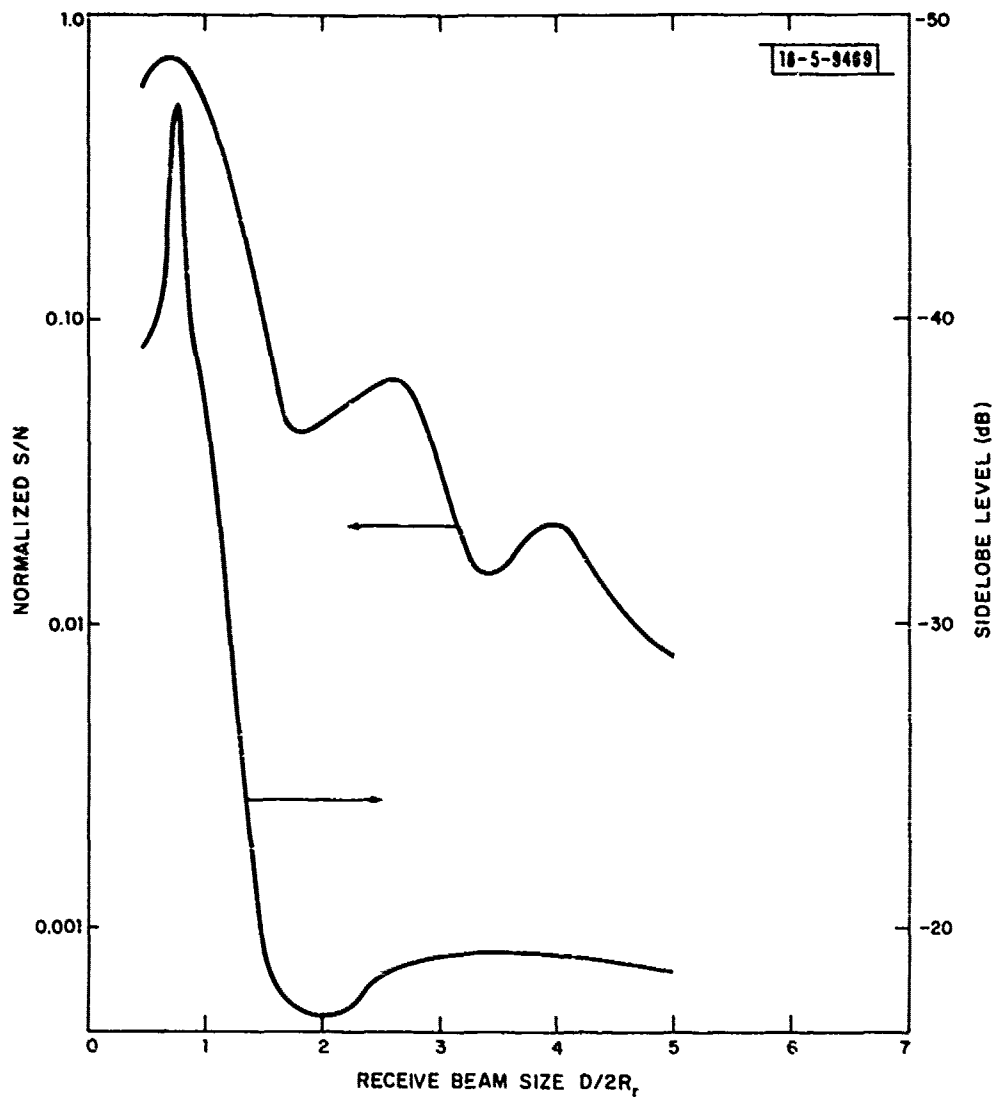


Fig. 18. Efficiency and sidelobe level for a uniform LO at the detector vs receive beam size.

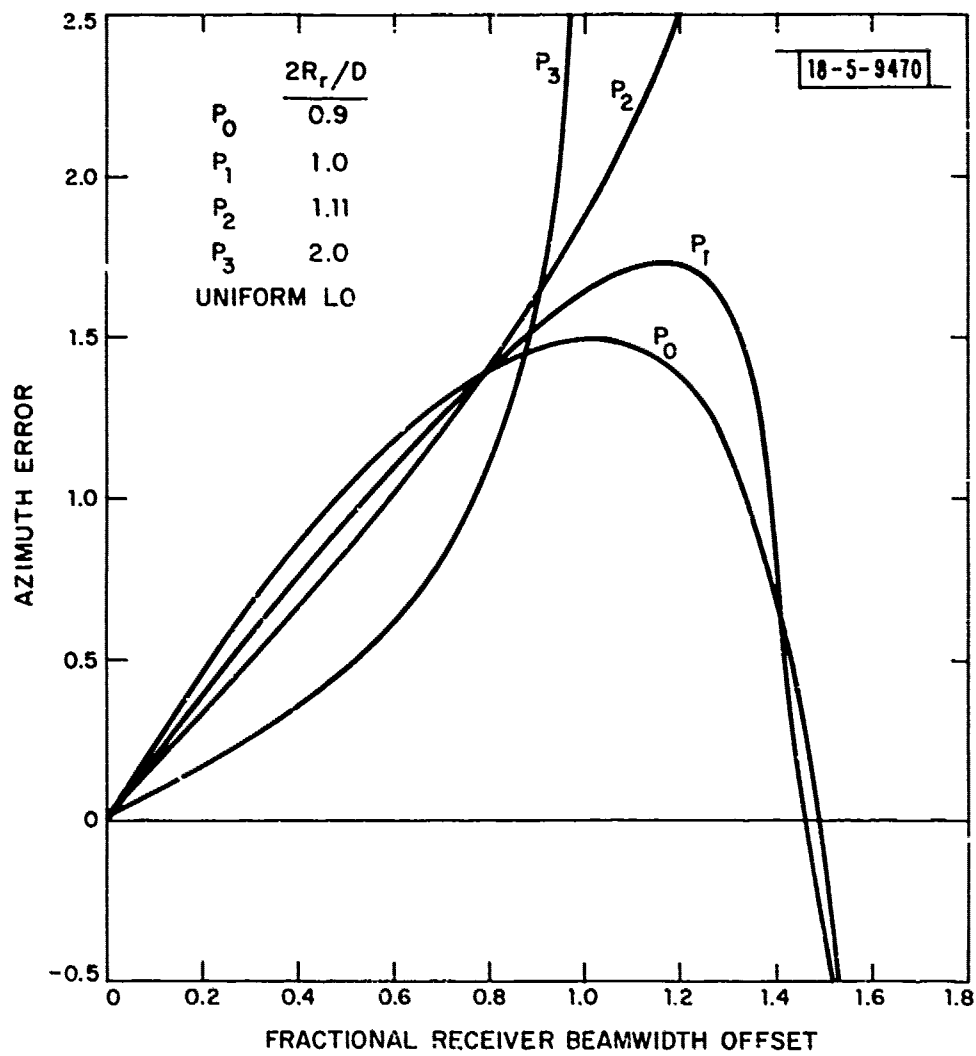


Fig. 19. Normalized azimuth errors for a uniform LO and various receive beam sizes.

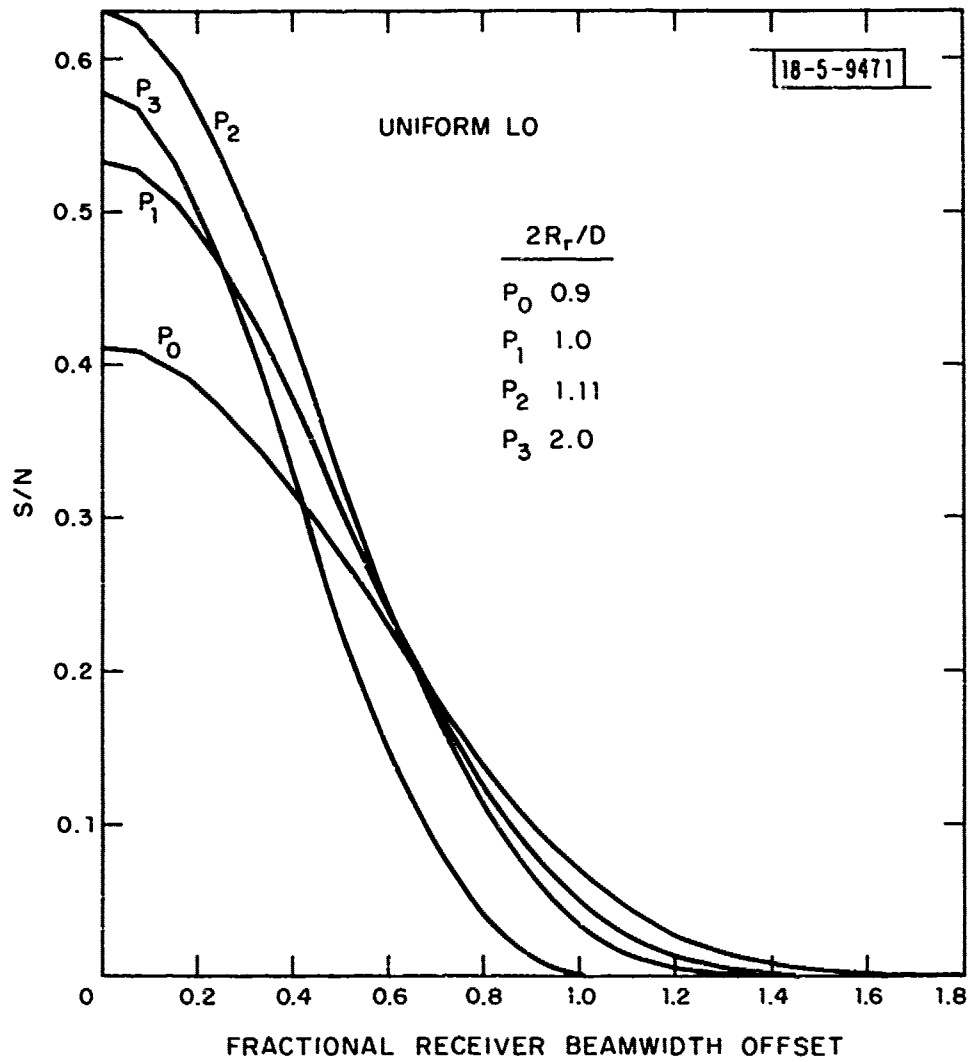


Fig. 20. Normalized signal-to-noise ratio for the cases considered in Fig. 19.

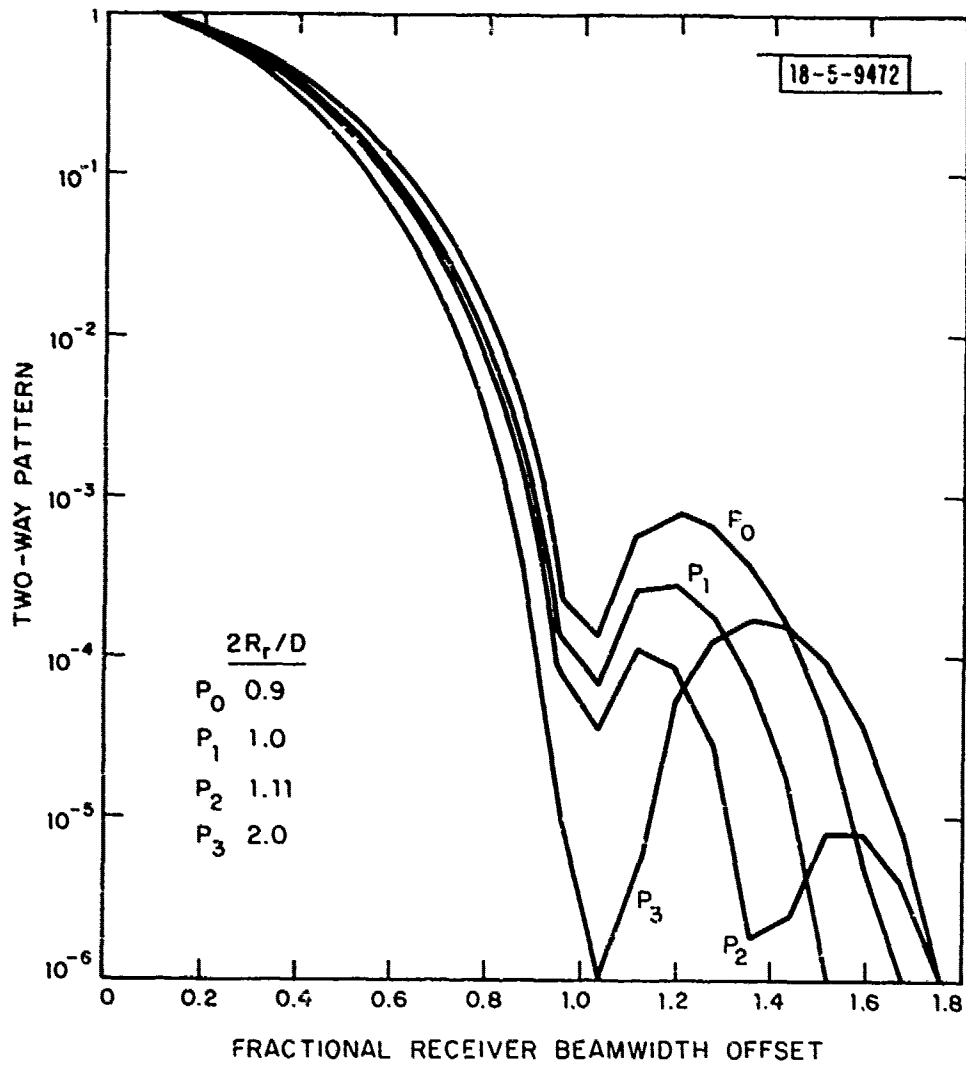


Fig. 21. Normalized two way pattern for the cases considered in Fig. 19.

sidelobe level. The off axis azimuth and elevation monopulse curves for elevation offsets of 0, .2, .4, .6, .8 and 1.0 beamwidth are shown in Figures 22 and 23, respectively. The curves are quite good.

F. Large Angle Search

It is desirable to be able to occasionally search in angle over areas larger than a beamwidth in a single PRI. There are problems in spreading the transmit beam uniformly over the areas to be searched. We will not discuss this but will concentrate on how the receive beam angle could be increased most efficiently.

A straightforward way of increasing the receive beam search angle is to decrease the spot size of the receive beam on the detector. Figure 24 is a plot of the monopulse pattern out to 4 beamwidths offset from boresight for a uniform LO distribution and receive beams whose distance between zeroes is one-half, one-third, one-fourth and one-fifth the detector size. One sees that the monopulse errors can be the proper sign for many beamwidths using this approach.

Of course, another major concern is the signal-to-noise ratio when this strategy is followed. Figure 25 is a plot of $(S/N)_N$ for these cases. On boresight there is very little difference in the $(S/N)_N$ cases of the receive beam being one-half or one-third the detector size. Also for the former case, the $(S/N)_N$ is considerably higher off axis. The reason for this behavior

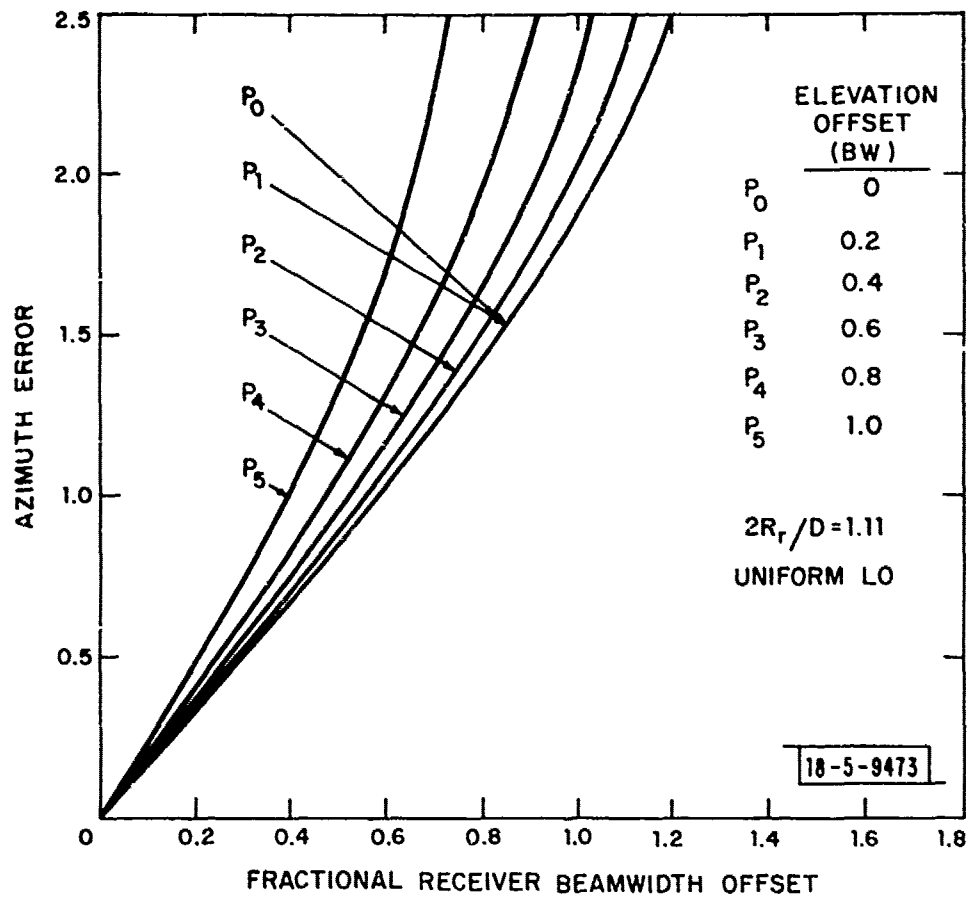


Fig. 22. Normalized azimuth error curves for a uniform LO with the receive beam 1.11 times the detector size.

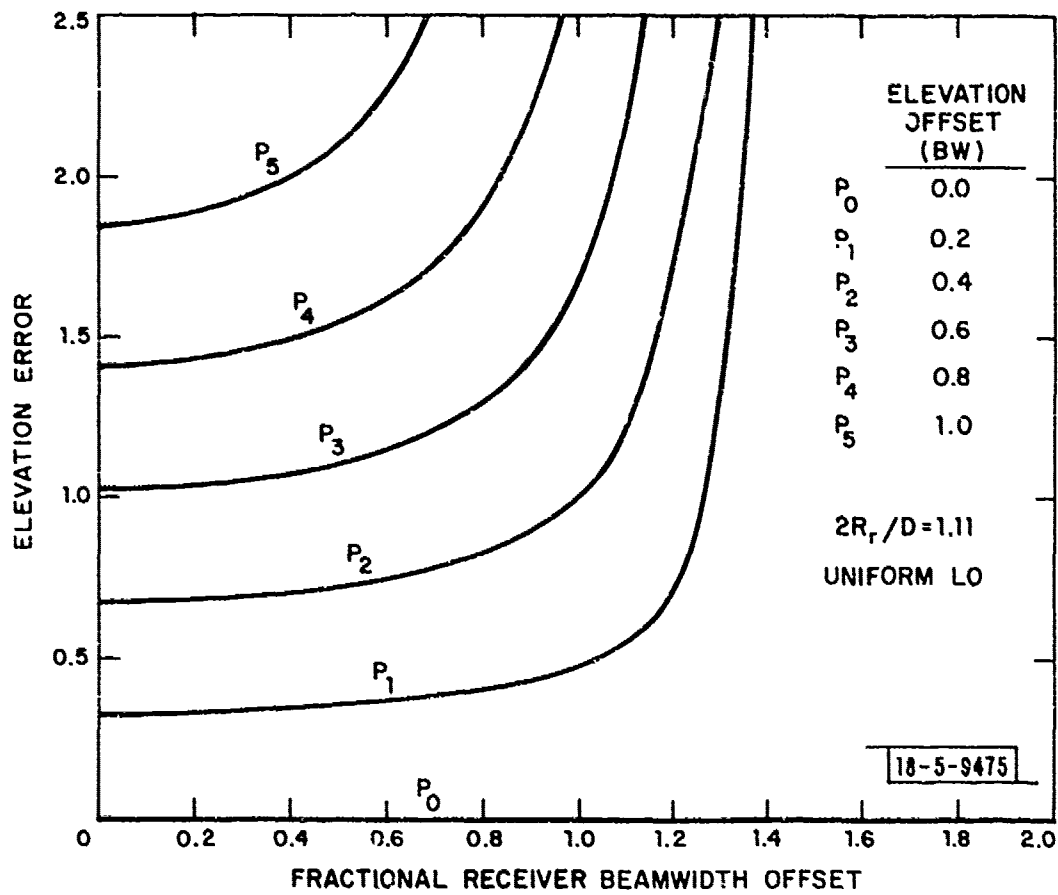


Fig. 23. Off axis elevation curves for a uniform LO with the receive beam 1.11 times the detector size.

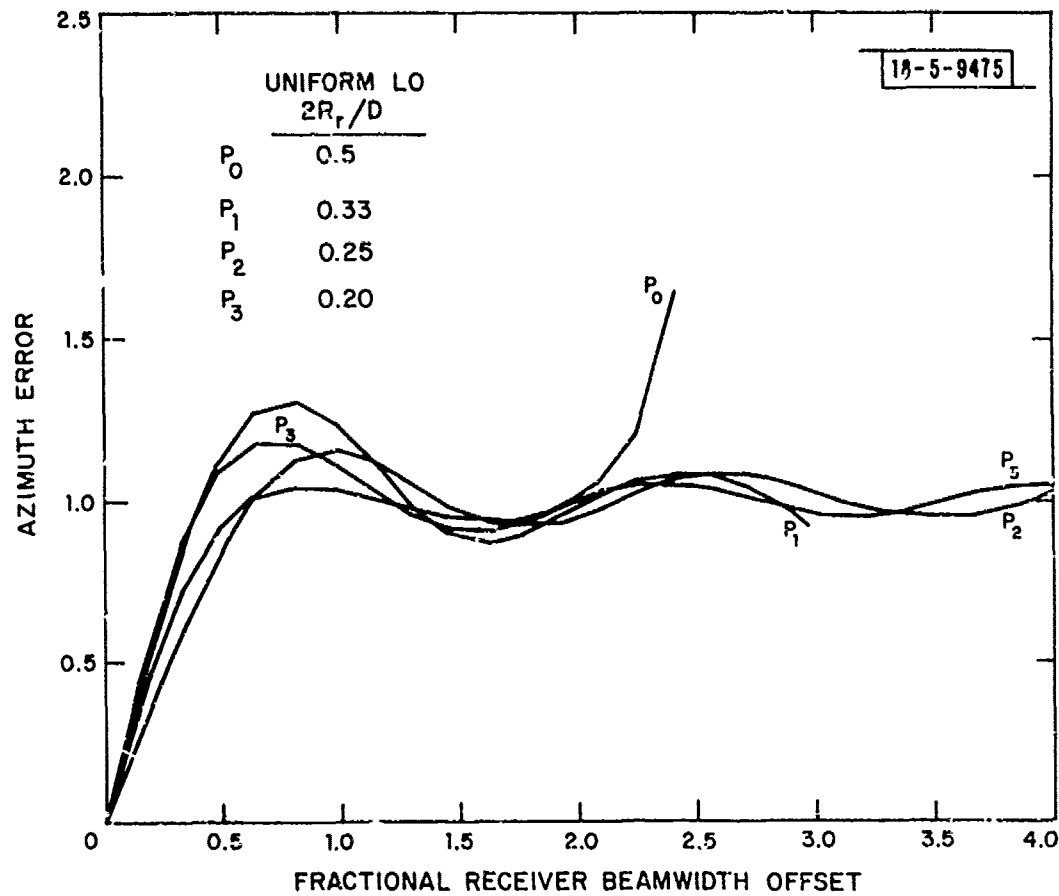


Fig. 24. Normalized monopulse patterns for a uniform LO distribution for receive beam sizes considerably smaller than the detector.

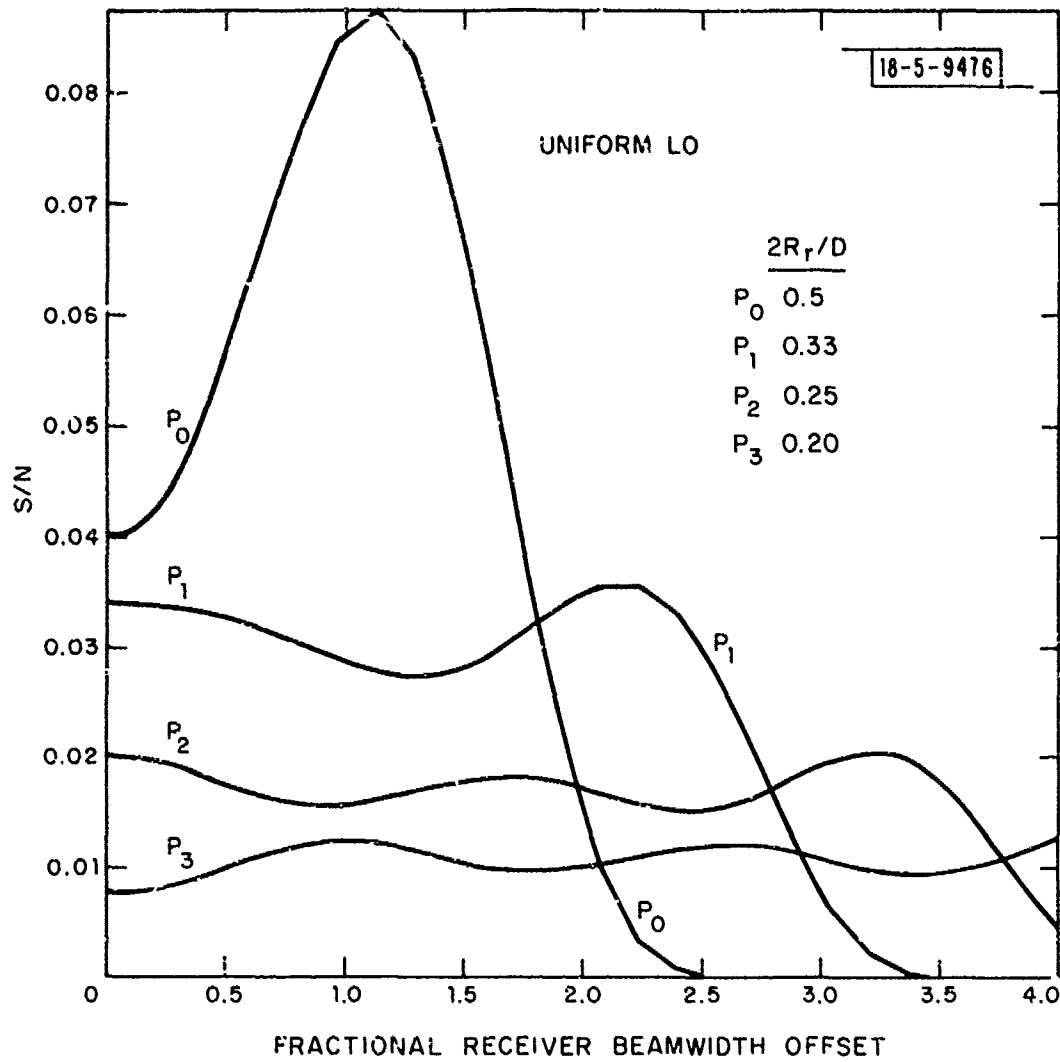


Fig. 25. Normalized signal-to-noise ratios for the cases in Fig. 24.

is that when the receive beam is one-half the detector size, the first sidelobe of the pattern is completely on the detector. The negative contribution of this sidelobe effectively cancels a large portion of the main lobe contribution. The major reason for this is that although the power in the first sidelobe is much less than the main beam, the detector responds to the field which differs as the square root of the power density. As the beam is moved off axis, the first sidelobe falls off the detector on one side while the second sidelobe which adds to the mainlobe contribution moves onto the detector. This explains the peculiar behavior.

From Figure 25, one sees that if the receive beam is one-third the detector size then one can get ± 2.5 beamwidths coverage with a loss of about a factor of 30 in S/N from the theoretical maximum. This increases the coverage by a factor of 25 in solid angle. To this must be added the transmitter pattern loss which will be at least a factor of 25 in some places in the beam.

Although the above approach is straightforward, the detector loss is excessive. The loss comes from the noise generated by the LO over a large area while the receive beam falls on only a small part of the detector. A way of reducing this loss is to break the detector into many separate elements and build a receiver channel for each element. Combining the output of many elements immediately after the detector does no good and essen-

tially brings one back to the case already considered. Therefore, to gain sensitivity requires many separate receiver channels.

If the receive beam size is comparable to the size of a detector element, then most of the receiver loss can be eliminated. No matter how many detector elements there are, one is confronted with the straddling loss. This loss results from the receive beam straddling as many as 4 detectors at some receive angles. In this case, the loss can be greater than 10 dB due to splitting the receive energy among 4 detectors and the sidelobes falling on the detector. Although this loss can be reduced by using combining circuits, the complexity of this approach probably would not be warranted. Therefore, using separate detectors in order to increase the solid angle search capability by a factor of N , one will suffer a loss due to increasing the size of the transmit beam plus straddling loss. It is necessary in this case to build an N element detector and N channel receiver with the proper detection logic.

IV. EFFECT OF TURBULENCE

When one is considering the placement of a feature to a small fraction of a beamwidth using the monopulse returns, then it is important to consider the effect of turbulence on those characteristics. Turbulence can change the average monopulse characteristic and also produce fluctuations about the average value.

The effect of turbulence will first be felt in disturbing the sidelobe pattern of the receive beam. Since the sidelobes affect the pattern greatly at larger off boresight angles, one would expect to first notice changes in slope and angle fluctuations at these angles. The quantitative effect of turbulence on the monopulse patterns has not been determined.

V. CONCLUSIONS

The cases of the LO distribution being uniform, Gaussian and Airy have been analyzed for a wide variety of sizes relative to the detector. Numerical values of quantities of interest such as monopulse slope, tracking errors versus S/N, detection loss, receive beam pattern, two way pattern and sidelobe level have been determined.

The optimum values of the different parameters are close in value for the various LO distributions. The signal-to-noise ratio is slightly lower for the uniform LO distribution.

Wide angle search with a heterodyne system incurs losses greater than 10 dB more than one would expect solely from spreading the transmit beam even if one increases the complexity of the receiver by having a separate channel for each additional detector element.

ACKNOWLEDGMENT

I would like to thank Joseph Alves for writing the plotting package used in this technical note.

REFERENCES

1. M. Born and E. Wolf, Principles of Optics (Pergamon Press, New York, 1964), p. 396.
2. J. J. Degnan and B. J. Klein, Appl. Opt. 13, 2397(1974).
3. D. K. Barton, Radar System Analysis (Prentice-Hall, Englewood Cliffs, New Jersey, 1964), p. 282.

APPENDIX A

WAVEFRONT TILT AT FOCUS

It will be shown that the wavefront tilt at focus is zero, regardless of the incoming wave tilt, if the input aperture is located at the focal plane of the input side of the lens and is centered on the optic axis as depicted in Figure 26. This statement and the proof of it given here are due to W. J. Scouler.

Consider the situation in Figure 26. A tilted wavefront passes through the aperture and is focused by the lens. Consider the central ray of the input wavefront 123. Since this wave passes through the focal point at 1, it is collimated by the lens and it is not tilted at focus. There are an equal number of rays symmetric about this central ray so the central ray determines the tilt of the wavefront at focus. Sometimes it is said that the central ray through the lens determines the tilt at focus. This is only true if the illumination on the lens is symmetric which is not true in our case.

18-5-9477

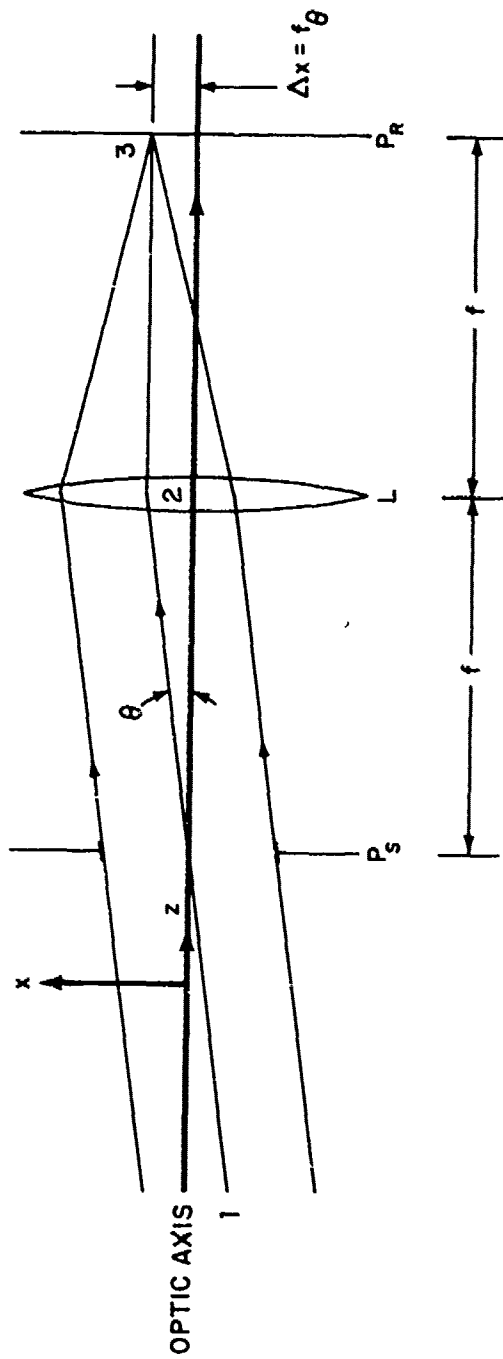


Fig. 26. Geometrical optics representation of detector optics.

UNCLASSIFIED

SECURITY CLASSIFICATION OF THIS PAGE (When Data Entered)

19 REPORT DOCUMENTATION PAGE		READ INSTRUCTIONS BEFORE COMPLETING FORM
1. REPORT NUMBER 18 ESD-TR-78-376	2. GOVT ACCESSION NO.	3. RECIPIENT'S CATALOG NUMBER
4. TITLE (and Subtitle) 6 The Monopulse Performance of an Optical Heterodyne Detector with Varying LO Distributions *		5. TYPE OF REPORT & PERIOD COVERED 9 Technical Note 19 TN-1
7. AUTHOR(s) 10 Richard J. Sasiela		8. CONTRACT OR GRANT NUMBER(s) 15 F19628-78-C-0002
9. PERFORMING ORGANIZATION NAME AND ADDRESS Lincoln Laboratory, M.I.T. P.O. Box 73 Lexington, MA 02173		10. PROGRAM ELEMENT, PROJECT, TASK AREA & WORK UNIT NUMBERS ARPA Order-600 Program Element No. 62301E Project No. 9E20
11. CONTROLLING OFFICE NAME AND ADDRESS Defense Advanced Research Projects Agency 1400 Wilson Boulevard Arlington, VA 22209		12. REPORT DATE 11 21 December 1978
14. MONITORING AGENCY NAME & ADDRESS (if different from Controlling Office) Electronic Systems Division Hanscom AFB Bedford, MA 01731 12 63 p.		13. NUMBER OF PAGES 64
		15. SECURITY CLASS. (of this report) Unclassified
		15a. DECLASSIFICATION DOWNGRADING SCHEDULE
16. DISTRIBUTION STATEMENT (of this Report) Approved for public release; distribution unlimited.		
17. DISTRIBUTION STATEMENT (of the abstract entered in Block 20, if different from Report)		
18. SUPPLEMENTARY NOTES None		
19. KEY WORDS (Continue on reverse side if necessary and identify by block number) IR radar monopulse performance receive beam angular coverage optical heterodyne detector transmit-receive beam pattern varying local oscillator distributions		
20. ABSTRACT (Continue on reverse side if necessary and identify by block number) Calculations are performed to determine the monopulse characteristics, the signal-to-noise ratio, efficiency, and the transmit-receive pattern of an optical heterodyne detector composed of four quadrants. The variation of these quantities for a varying receive beam size on the detector, and a uniform LO, and Gaussian and Airy LO distributions of varying size are tabulated. The calculations are applied to determine the possibility of increasing the angular coverage of an optical heterodyne receiver.		

207 650

4/B